Fluid Dynamics &
Materials Processing

Tech Science Press

Doi:10.32604/fdmp.2025.069428

REVIEW

3D Printing of Organic and Biological Materials

Priyadarshini Patel and Komal Parmar*

ROFEL Shri G.M. Bilakhia College of Pharmacy, Rajju Shroff ROFEL University, Vapi, 396191, India
*Corresponding Author: Komal Parmar. Email: komal.parmar2385@gmail.com

Received: 23 June 2025; Accepted: 26 December 2025; Published: 31 December 2025

ABSTRACT: Tissue engineering has advanced remarkably in developing functional tissue substitutes for pharmaceutical and regenerative applications. Among emerging technologies, three-dimensional (3D) printing, or additive manufacturing, enables precise fabrication of biocompatible materials, living cells, and scaffolds into complex, viable constructs. Within regenerative medicine, 3D bioprinting addresses the growing demand for transplantable tissues and organs by assembling biological materials that replicate native architectures. This paper reviews biomaterials used in 3D bioprinting, emphasizing how their rheological behavior, particularly viscoelasticity and thixotropy, governs printability, structural fidelity, and cellular viability. The advantages and limitations of natural, synthetic, and composite bioinks are analyzed in relation to their mechanical performance and flow properties. In addition, common 3D bioprinting techniques such as extrusion, inkjet, and laser-assisted methods are outlined with reference to their compatibility with various material systems. Recent applications in bone, cartilage, vascular, skin, neural, cardiac, hepatic, and pulmonary tissue engineering are briefly summarized.

KEYWORDS: 3D bioprinting; biomaterials; scaffolds; tissue engineering

1 Introduction

The advent of the printing press altered human history. The revolutionary technique of printing text and images had a global influence, serving as a medium for education, religion, politics, language, and culture [1]. Numerous developments since then have improved printing processes much further. The consumer market was transformed, for instance, by the advent of dot matrix printers, which reduced costs and time by enabling desktop publishing and on-demand printing via a computer connected to a printer as a peripheral device. The general public now has more access to education, scientific research, and the arts due to personalized printing.

In recent years, additive manufacturing (AM) has gained significant attention. Additive Manufacturing (AM) is recognized as a noteworthy sustainable manufacturing technology [2]. Numerous industries, including engineering, architecture, medicine, industrial design, construction, and many more, have discovered broad uses for 3D printing, the process of producing a three-dimensional product from a computer-driven digital model [3]. Three-dimensional (3D) printing, sometimes referred to as additive manufacturing (AM), layered manufacturing, rapid prototyping (RP), or solid freeform fabrication, is the process of directly fabricating parts one layer at a time using digital data from a computer-aided design (CAD) file without the need for part-specific tools. In 3D printing, CAD models of the objects that need to be created are first sliced in a virtual environment to generate a stack of two-dimensional (2D) slices. Based on the 2D slice information, a 3D printer then constructs the components one layer at a time, stacking and combining subsequent layers to create the finished 3D product [4,5]. Unlike mass production, it enables individuals to make personalized things on demand at

cost-effective pricing. The rapid spread of this technology can be attributed to cost reductions that make it advantageous for producing certain product categories, such as those made in limited quantities, require personalization, or are not possible to manufacture using traditional manufacturing methods. Technology has become widely used in several industries, leading to the third industrial revolution [6]. Applications for 3D printing are widespread in a wide range of industries, including the food industry, biotechnology, biomedical, and analytical fields. It has been reported that 3D printing can be used to visualize molecules and proteins, as well as to teach about orbitals and surfaces [7].

Bioprinting is made feasible by the capability of a 3D printer to dispense biological materials. Bioprinting is described as: "the utilization of material transfer techniques for designing and assembling biological relevant materials, molecules, cells, tissues, and biodegradable biomaterials—using predefined architecture to execute one or more biological functions" [8,9]. Biomaterials and living cells can typically be positioned layer by layer to accomplish bio-printing. 3D tissue architectures, including skin, cartilage, tendons, heart muscle, and bone, may be created because of the functional materials' exquisite spatial control. The first step in the procedure is choosing the appropriate cells for the tissue [10]. Patient-specific treatments are crucial in the biomedical industry to enhance biological repair, replacement, and regeneration [9]. With programmable micro-architecture, 3D printers may create custom structures for each patient using clinical image data from X-rays, magnetic resonance imaging (MRI), or computerized tomography (CT) scans [11,12]. For instance, utilizing 3D printing and CT scans of the patient's airway, medical professionals recently designed a biodegradable tracheal splint for a baby. Additional examples include medicine delivery implants, customized medications, and printed artificial ears made especially for individuals [13,14]. 3D printing is a cost-effective and time-saving alternative to traditional production methods for prosthetic implants [15].

Printing scaffolds, which serve as supports for developing cells, is one technique of bioprinting. This enables the precise placement of biomaterials, live cells, growth agents, and other biological elements for generating complex 3D living tissue [16]. Scaffolds are essential for tissue engineering as they offer the following: extracellular matrix production and remodeling space, structure for cell infiltration and proliferation, biochemical signals to guide cell activity, and physical connections for wounded tissue. Designing scaffold architecture at the macro, micro, and nano levels is crucial for optimal structural, nutrient transport, and cell-matrix interaction conditions. The macroarchitecture refers to the device's overall form, which might be complicated due to patient and organ specialization and anatomical factors. The tissue architecture (including pore size, shape, porosity, spatial distribution, and pore connections) is reflected in the microarchitecture. Nanoarchitecture involves surface modification, such as biomolecule attachment, to promote cell adhesion, proliferation, and differentiation [17].

While an ideal scaffold should address all of these criteria, difficulties persist with biomaterial selection and 3D shape specificity. Commonly utilized biomaterials include synthetic and natural polymers, ceramics, metals and carbon based nanomaterials. Each biomaterial has unique material and mechanical qualities, manufacturing techniques, chemical properties, cell-material interactions, and approval from the FDA [18]. Bioprinting technologies have made significant contributions to biomedical research, although they are still in their early stages of development [19,20]. Developing scaffolds for high load bearing applications presents challenges due to the limited biodegradability and bioactivity of current printable materials like ceramics and metals, as well as the potential for inflammatory responses from host tissues. Furthermore, metals and ceramics cannot be functionalized with drugs or biomolecules.

Using organic materials in the form of powders can help produce scaffolds with acceptable mechanical characteristics, biodegradability, biocompatibility, and bioactivity [21,22]. Polymers (macromolecules) are the major scaffolding materials used in a variety of tissue engineering applications, including bone and mineralized tissues [23,24]. BioPolymers are a remarkable choice for tissue engineering applications, thanks

to their adaptability and the extensive variety of mechanical, chemical, and physical characteristics they can deliver. These materials demonstrate high biocompatibility, are lightweight, inert, and are resistant to biochemical assaults and are easily available at affordable prices and can be rapidly shaped into the desired forms. Polymeric biomaterials may originate from both natural and synthetic polymers, each having its own set of advantages and disadvantages. Natural polymers include proteins such as collagen, elastin, keratin, gelatin, and fibrin, along with carbohydrates like chitin, cellulose, starch, alginate, and hyaluronic acid; synthetic polymers include polyesters such as poly ε-caprolactone, polylactic acid, and polyglycolic acid [25,26].

Even though three-dimensional (3D) printing was initially introduced in the late 1980s using a process known as stereo lithography, its importance didn't become apparent until the turn of the twenty-first century [27]. Stereolithography (SLA), the earliest additive manufacturing (AM) technique, was first invented in 1981 by Dr. Hideo Kodama. In contrast to holographic methods, he considered it a quick and inexpensive way to recreate models in 3D space [28]. Several 3D printing techniques have been explored since the first stereolithographic 3D printer was invented in 1986 by Chuck Hull, the most common being fused deposition modeling (FDM), stereolithography (SLA), selective laser sintering (SLS), selective laser melting (SLM), electronic beam melting (EBM), digital light processing (DLP), and laminated object manufacturing (LOM). Their goal was to make it easier to quickly prototype plastic components [29]. SLA has greatly expanded beyond its initial applications in modeling and prototyping with the invention of several techniques, and it can now be used to build intricate and custom-designed geometries. The material is no longer confined to traditional polymers, but may also be used to generate composites [30], metallic [31], and ceramic [32] specimens. However, SLA is currently only being used to build one material at a time, and when compared to other AM technologies, typical SLA techniques demonstrate improved resolution and surface characteristics, but at a higher cost and slower printing durations [33].

The actual printing of the bioink utilizing the bio-printers is known as the processing stage. In order to generate the required biological structures, the processing step involves the development of bioink, clinical cell sorters (like Celution and Cytori Therapeutics), cell propagation bioreactors (like Aastrom Bioscience), and cell differentiators.

During the post-processing phase, the printed construct is converted into a functioning tissue-engineered organ that may be surgically implanted. Cell encapsulators, perfusion bioreactors, and a collection of bio-monitoring devices may also be employed in the postprocessing phase [34].

The aim of this review is to provide a comprehensive overview of the current state of bioink technology. The review covers both natural and synthetic biomaterials, employed alone or in combination. This paper will also review sophisticated techniques for 3D printing used for developing tissue engineering scaffolds, with a focus on their capacity to design cells and various materials along complex 3D gradients.

2 Characteristics of Biomaterials and Biomaterial Scaffolds

Biomaterials are natural or synthetic materials that repair injured body components and interact with biological systems. Innovative biomedical devices to enhance human life have been developed during the past century with the advent of metallic, ceramic, and polymeric biomaterials [35]. To be effective, these substances must not be harmful and must be compatible with the tissues of the body. Three-dimensional (3D) porous biomaterials known as scaffolds offer an ideal platform for cells to regenerate and repair tissues and organs [36]. In addition to encouraging cell attachment, proliferation, extracellular matrix regeneration, and the repair of nerves, muscles, and bones, it acts as a template for the rebuilding of tissue defects. Furthermore, as a mechanical barrier against the invading native tissues, scaffolds can carry bioactive substances, including medications, inhibitors, and cytokines, which might impede tissue regeneration

and repair [37]. The success of generating biomedical scaffolds depends on the choice of biomaterials. The scaffolds must have comparable properties that match the application at hand and be specifically built to perform specific functions. These characteristics fall under the categories of mechanical qualities, biodegradability, biocompatibility, and structural architecture as displayed in Fig. 1.

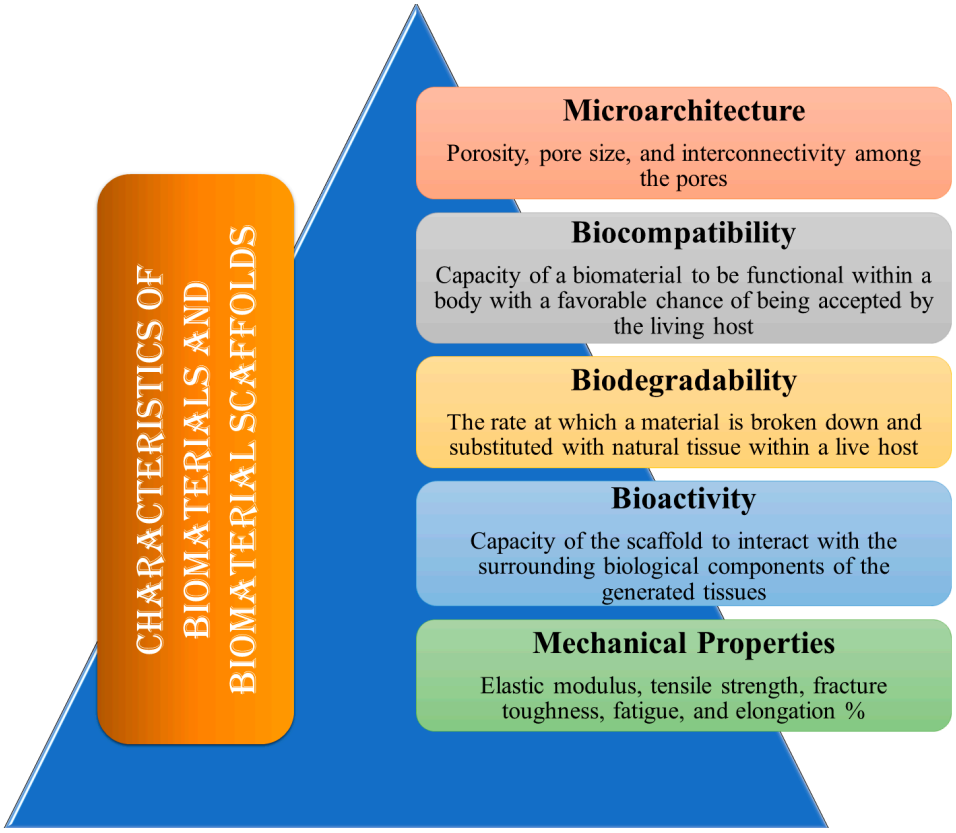

Figure 1: The ideal features of biomaterials and biomaterial scaffolds.

2.1 Microarchitecture

Porosity, pore size, and interconnectivity among the pores are all components of the scaffold's microarchitecture. Primarily, the size of the pores must be adequate to facilitate cell motility and scaffold attachment. This provides adequate vascularization and infiltration, as well as the efficient movement of waste products and nutrients into and out of the cells and tissues. For *in vitro* applications, a smaller pore size of 75 to 100 μm is recommended, while *in vivo*, the maximum pore size should be between 200 and 500 μm to achieve the most effective tissue penetration and vascularization [38,39]. Additionally, to augment the scaffold surface area that supports cell adhesion, a network of interconnected pores is required. Greater porosity aids in the integration of the designed tissues with the natural tissues by improving cell-to-cell connections [40].

2.2 Biocompatibility

The capacity of a biomaterial to be functional within a body with a favorable chance of being accepted by the living host is the single most significant characteristic that distinguishes it from a normal material. The ability of a biomaterial to work in conjunction with a medical therapy, producing the best possible cellular and tissue response in the specified anatomical site, optimizing the effectiveness of

the medical treatment, and avoiding any undesirable local or systemic effects on the recipient is termed biocompatibility [41]. Biocompatibility refers to a material that is safe for humans and has the necessary properties for medical applications, such as mechanical properties and degradability, while remaining non-toxic and non-carcinogenic. The scaffold must exhibit a high degree of biocompatibility to facilitate cell adhesion and proliferation, while also minimizing chronic immune responses to avert significant inflammatory reactions that could hinder healing or lead to rejection within the body [42,43].

2.3 Biodegradability

Biodegradability refers to the rate at which a material is broken down and substituted with natural tissue within a live host. By-products are absorbed and released by the body's metabolic processes [44]. Scaffolds should be gradually broken down chemically or enzymatically when transplanted into living organisms, since they serve only as a transitory platform for growing cells or tissues. Biodegradability is the rate at which the scaffold materials decompose. The scaffold's rate of biodegradation needs to be proportionate to the pace of tissue regeneration or new bone development. Through a process known as "creeping substitution," newly generated tissues will eventually replace the biomaterial scaffolds after they have been effectively integrated with the host bone. The mechanical properties and structural integrity of a biomaterial during its entire lifespan are also described by its biodegradability, which in turn indicates the kind of application for which the biomaterial is appropriate [45].

2.4 Mechanical Properties

Biomaterial scaffolds must possess a certain level of mechanical integrity in relation to their intended use. Preferably, structures ought to possess the same consistency as the anatomical location where they are situated into, yet sufficiently robust to be handled and inserted [46]. There are differences in the mechanical characteristics of tissue. In addition to offering form stability and structural support, it also reduces the chance of stress shielding, implant-related osteopenia, and future refracture. In furtherance of necessitating the appropriate mechanical characteristics to support heavy load bearing applications, these scaffolds also must stay in perform until the healing process has been completed [46,47]. Elastic modulus, tensile strength, fracture toughness, fatigue, and elongation % are a few examples of mechanical characteristics [48].

2.5 Bioactivity

The capacity of the scaffold to interact with the surrounding biological components of the generated tissues is known as scaffold bioactivity. Bioactive scaffolds are intended to promote appropriate cell migration or differentiation, tissue regeneration or neoformation, and host integration, thereby preventing processes like scarring, in contrast to conventional passive biomaterials, which typically have minimal or no interactions with the environment [39]. Scaffolds can be affixed to physical markers like topography to improve cell morphology and alignment, or they can be affixed to cell-adhesive ligands to encourage cell adhesion. Furthermore, to promote tissue regeneration, bioactive scaffolds may act as a reservoir or transporter for growth-stimulating stimuli like GFs [49].

3 Materials/Biomaterials Utilized for 3D Bioprinting

Current scaffold research confronts the problem of developing materials with good mechanical integrity for high load bearing applications while preserving optimal levels of biodegradability, biocompatibility, and bioactivity. Scaffold material selection should be based on the patient's condition. Those with cancer or osteoporosis often experience diminished bone metabolism, thus it is essential that the scaffold material is not resorbable. Scaffolds are typically constructed from four categories of biomaterials: polymers,

bio-ceramics, metals, and carbon nanomaterials. These scaffolds can incorporate various biomaterials owing to their distinct advantages and disadvantages. Currently, carbon-based nanomaterials, bioceramics, biodegradable metals, as well as both natural and synthetic polymers, among other materials, are utilized in the development of scaffolds [50].

3.1 Polymers

Polymers are among the most often utilized materials for bioink. Because of their affordable cost, biocompatibility, degradation, and safe processing, polymer bioinks are employed in bioprinting. The capacity of polymer bioinks to alter shape is one of their additional benefits. For instance, they can be utilized as powders for laser bioprinting or as filaments for fused-deposition modeling. Polymeric biomaterials, which are essential components in many biomedical applications, come from two sources: naturally occurring polymers and synthetically engineered polymers. Each category has a distinctive combination of benefits and drawbacks that determine its applicability for various applications [25]. Artificial organs and blood arteries, breast implants, contact lenses, coatings for pharmaceutical tablets and capsules, joint replacements, cardiac assist devices, and external and internal ear repairs are a few biomedical applications employing polymers.

3.1.1 Natural Polymers

Natural polymers are non-toxic, biocompatible, attach well to cells, and promote proliferation and differentiation. However, they lack mechanical strength and are vulnerable to high temperatures [51]. Natural polymers are derived from natural sources. They fall into two categories: biomaterials based on proteins (which are naturally occurring polymers in the human body, like collagen, fibrin, and elastin) and biomaterials based on polysaccharides (which include silk, chitosan, alginate, and gelatin). Their properties are similar to those of soft tissues, demonstrating bioactivity, better cell growth and adhesion, and meeting biodegradability and biocompatibility requirements. They are also renowned for being widely accessible, environmentally safe, and adaptable to many uses. Nonetheless, natural sources suggest that a purification phase is necessary to prevent post-implantation foreign immune response. Furthermore, natural polymers usually exhibit low mechanical and physical stability, which restricts their use in the load-bearing orthopedic industry [24].

Collagen

Collagen is a biocompatible polymer that has been extensively studied in bioprinting and, more specifically, tissue engineering. It is the predominant constituent of musculoskeletal tissue and constitutes the extracellular matrix of the majority of tissues. In reality, collagen is a naturally occurring triple-helical biocompatible protein. As a result, collagen scaffolds cause low immunological responses. In addition, collagen can promote cell proliferation, adhesion, and attachment. Although collagen type 1 has been widely employed in 3D printing, it has limits [52]. Three alpha helices combine to produce a triple helical shape in type I collagen, which is a member of the fibril-forming collagen group. Collagen molecules begin to organize themselves into fibrils at physiological temperatures (37°C and neutral pH), and the collagen solution turns into a hydrogel. Collagen bioink printability is dependent on the kinetics of this process; the faster the process, the more accurate the print [53].

Hyaluronic Acid

Hyaluronic acid (HA) is a naturally occurring polymer found in the extracellular matrix of numerous tissues that is not immunogenic. It can control a wide range of cell behaviors and tissue functions and

has outstanding hydrophilicity and biocompatibility [54,55]. However, HA by itself is not a good bioink for 3D bioprinting because of its low mechanical strength and rapid rate of breakdown. In addition, the concentration of the component may be changed to modify the hydrogel's mechanical characteristics [56]. The researchers chemically modified HA and combined it with a printable hydrogel to create an HA-based hydrogel solution. In contrast to pure HA and/or other hydrogels, the solution demonstrated not only high biocompatibility and biodegradability, but also the mechanical strength and stiffness needed for bioink applications. HA-based hydrogel solutions are currently gaining popularity as bioinks, with promising future applications in the bioprinting of skin, nerve tissue, cartilage, and bone [57,58].

Fibrin

Fibrin is a vital protein for blood clotting and wound healing. These proteins play critical roles in neoplasia, cell-matrix interactions, and inflammatory responses. Fibrinogen, a glycoprotein generated by the liver, rises in response to trauma. Thrombin, a serine protease produced after arterial injury, hydrolyzes fibrinogen and polymerizes it into fibrin. Fibrin is a scaffolding material commonly utilized in tissue engineering, notably for vascular grafts. Fibrin gels (gelation time is rapid) provide desirable properties, including differentiation, biodegradability, promote cell proliferation, angiogenesis, biocompatibility, and regeneration of tissues. Additional benefits of fibrin include its superior mechanical qualities, heparin-binding domains with affinity for growth hormones, and binding sites for natural extracellular matrix proteins [59]. A fibrin-gelatin hybrid hydrogel was utilized as biopaper for skin bioprinting. Fibrin-factor XIII-hyaluronate hydrogel scaffolds were used in an *in vitro* study to encapsulate Schwann cells, potentially improving nerve regeneration and repair [60].

Chitosan

Chitosan, a polycationic biocompatible natural polymer, has certain distinct advantages for bioprinting applications. Solutions containing chitosan exhibit suitable viscosity profiles and maintain stability in physiological environments, making them suitable for use in bioprinting applications. Additionally, chitosan promotes healthy cell differentiation and proliferation. High vitality is demonstrated by cells grown on chitosan scaffolds. As a result, chitosan hydrogels and resins satisfy these criteria; moreover, chitosan hydrogels may be adjusted to effectively replicate the natural extracellular matrix (ECM) of tissues [61]. However, in tissue engineering, this natural polymer has demonstrated several limitations, such as poor mechanical strength and a sluggish gelation rate. It is important to remember that a bioink must be a liquid or semi-solid substance that may be crosslinked chemically or physically in order to have mechanical strength and physical stability. Therefore, to increase the likelihood of stronger crosslinking, chitosan-based biomaterials can be altered using a number of techniques, such as coupling with methacrylic anhydride (methacrylation of backbone). Because of its appealing set of qualities listed above, chitosan hydrogels are a preferred biomaterial for bioprinting, and crosslinking them helps to overcome their inherent slight drawbacks. As an outcome, chitosan and its derivatives are appropriate for tissue engineering applications such as replacing or repairing bone, cartilage, and skin. As natural biomaterials, chitosan-based bioinks are thought to be the best choice for designing and creating multiple scaffolds using 3D bioprinting because of their remarkable biological qualities and unique dynamic reversibility [62,63].

Gelatin

Gelatin, a protein derived from collagen, is shear-thinning, has cell-adhesive ligands, may be broken by cells enzymatically, and physically gels below room temperature. Gelatin bioinks have garnered a lot of interest in tissue development because of these properties. In order to find bioinks that support

certain cell types, many gelatin-based bioinks have been developed thus far. Gelatin-based bioinks have been used with a variety of encapsulated cell types (i.e., primary cells, stem cells, and cancer cells) and bioprinting processes (extrusion, droplet, and light/laser-based) [64]. While gelatin and collagen have a similar molecular makeup, gelatin has a less organized macromolecular structure and nevertheless contains crucial binding moieties for cell adhesion, such as the tripeptide Arg-Gly-Asp (RGD) sequence. Furthermore, it has peptide sequences that the matrix metalloproteinases (MMPs) enzymes may break and exhibits lower antigenicity than collagen. Gelatin's sensitivity to MMP allows it to be broken down by the MMP enzymes released by encapsulated cells, which promotes microenvironment remodeling. Additionally, gelatin has viscoelastic characteristics that support cell proliferation, differentiation, and migration. These qualities make gelatin one of the most popular natural biomaterials for bioprinting [65].

Silk

The FDA authorized the use of silk fibroin (SF), a natural polymer derived from the silkworm Bombyx mori, as a biomaterial in 1993. Because of its remarkable biocompatibility, adaptable mechanical characteristics, regulated biodegradation, and low tendency to elicit immunological responses, it has been widely used recently in the tissue engineering and biomedical domains. Gly–Ala–Gly–Ala–Gly–Ser repetitions of amino acid sequences make up SF, which self-assembles to create a β-sheet structure. SF has been shaped into a variety of shapes for a wide range of biomedical applications, including films, hydrogels, sponges, electrospun mats, and nano- or microparticles. Because of the versatility it offers, SF has been used as a major bioink material for a number of 3D printing techniques, such as extrusion-based and inkjet bioprinting [66]. However, SF's limited abundance and poor viscosity are major disadvantages for using it as a bioink for broad 3D printing applications. To improve its printability, SF is therefore being used as a bioink for 3D bioprinting by combining it with other high-viscosity materials. Adding more crosslinking to natural biomaterials is a popular tactic to enhance their mechanical qualities and printability. A cross-linking technique called photo-crosslinking has produced more intra- and intermolecular chemical connections, resulting in a quick and reliable cure [67].

Alginate

An inexpensive biopolymer, alginate—also known as algin or alginic acid—is typically made from calcium, magnesium, and sodium alginate salts found in the intracellular spaces and cell walls of various brown algae. Alginate is made up of β-d-mannuronic (M) and α-l-guluronic acids (G), which are (1–4) connected. Longer M or G blocks, separated by MG regions, form the polyanionic linear block copolymer known as alginate. Alginate is a negatively charged polysaccharide. This soluble biopolymer has excellent biocompatibility and promotes cell development. While MG and M blocks improve flexibility and G blocks boost gel formation, an excessive quantity of M blocks may result in immunogenicity. Capillary forces can trap water and other molecules in an alginate matrix while yet allowing them to disperse. This property qualifies alginate hydrogels for bioink compositions [68]. Numerous alginate-based inks have been documented, some of which are marketed commercially (e.g., "CELLINK") [69]. One of the most beneficial aspects of alginate is its adaptability to a range of bioprinting technologies (such as extrusion, inkjet, and microfluidic bioprinting) and scaffold construction techniques (such as spheroids, vascular constructs, and microfluidic fiber-shaped scaffolds) [70].

3.1.2 Synthetic Polymers

Synthetic polymers are man-made polymers with modifiable chemical structures and physical characteristics that are manufactured by chemical processes. In contrast to natural polymers, the majority

of synthetic polymers possess super mechanical features. Because 3D printing frequently uses organic solvents, heat, and toxic activators that may lessen the bioactivities of cells and growth factors, synthetic polymers are relatively bio-inert and cannot easily incorporate bioactive ingredients, such as cells and growth factors, directly. There are synthetic polymers that decompose naturally. *In vivo*, microbes or biological fluids can break down these polymers [71].

Polyethylene glycol (PEG), Polycaprolactone PCL, polyvinylpyrrolidone (PVP), poly(L-lactic) acid (PLA), Polyurethane (PU) and poly(lactic-co-glycolic) acid (PLGA) are examples of synthetic polymers that are often utilized in 3D bioprinting. They may be tailored to meet the mechanical property specifications for the target tissues and organs, as well as tissue-specific breakdown [72].

Synthetic polymers with appropriate mechanical qualities can tolerate internal and external stresses throughout the *in vivo* implantation and 3D printing phases. Therefore, as compared to natural polymers, the majority of synthetic polymers have several inherent benefits in the field of bioartificial organ 3D printing. Convenient synthesis, resource abundance, ease of processing, stress tolerance, light weight, and affordability are among the apparent benefits [71].

Despite this, they only make up around 10% of the systems utilized in bioprinting because of an assortment of drawbacks that prevent them from being employed in translational applications (hard to encapsulate cells, usage of toxic solvents, melting temperatures greater than body temperature). Furthermore, locations for cellular recognition and other biological signals present in natural extracellular matrix (ECM) that promote cellular proliferation and differentiation are typically absent from synthetic polymers. The existence of flexible side groups becomes necessary for appropriate customization of a construct's mechanical and biological features, even if functionalization of synthetic bioinks might enhance their biological qualities [72].

Polyethylene Glycol

PEG is a synthetic polyether that is inexpensive, soluble in organic solvents or aqueous solutions, and has a high degree of biocompatibility. PEG is widely used for wound dressing and medication administration because it has no negative effects on cell adhesion or proliferation. Cell adhesion can be improved by including cell-binding motifs into the PEG hydrogel network, such as arginylgly-cylaspartic acid (Arg-Gly-Asp) peptides [73].

Another work used polyethylene glycol diacrylate (PEGDA) and self-assembled peptide nanofibers to generate a hybrid bioink for 3D printing lumens. First, peptide-loaded 2D and 3D layers of adult human dermal fibroblast (aHDF) cells were seeded, and the behavior of the cells was examined. After being injected into the 3D hydrogel, the cells' shape remained spherical and closely matched that of the 2D overlay hydrogels. HDF cells were able to attach and multiply on PEGDA/peptide lumens but did not adhere to unmodified PEGDA lumens. Furthermore, a characteristic distributed F-actin shape was shown by HDF cells implanted on the hybrid PEGDA/peptide lumens [74].

Through the use of off-stoichiometry thiolene click chemistry, a novel PEG microgel was developed. It was readily extruded as bioink and demonstrated excellent stability following printing because of the intraparticle adhesion forces. In the end, the method generated printed structures with long-term stability and endurance and permitted a second thiolene click reaction. One benefit of this bioink is its modularity, which is a result of the versatile physicochemical features of PEG microgels. Since the cells could spread and multiply in the PEG micro-gel interstitial gaps, the bioink's low extrusion force and the thiolene annealing process enabled good cell survival during bioprinting [75].

Another study uses therapeutic protein-loaded nanoengineered bioink to control cell activity in a 3D-printed structure. A 2D synthetic nanoparticle and a hydrolytically degradable polymer are used to

develop the bioink. Acrylate-terminated degradable macromer is produced using a Michael-like step growth polymerization process used to synthesize poly(ethylene glycol)-dithiothreitol (PEGDTT). Shear-thinning bioinks with excellent printability and structural integrity are created when 2D nanosilicates are added to PEGDTT. Altering the PEG: PEGDTT ratio and the concentration of nanosilicates can modify the mechanical characteristics, swelling kinetics, and rate of degradation of 3D printed structures. Protein therapies may be contained in 3D printed structures for an extended period of time because of the large surface area and charged nature of nanosilicates. The fast migration of human endothelial umbilical vein cells was facilitated by the sustained release of pro-angiogenic therapies from 3D printed structures [76].

Polycaprolactone

The United States Food and Drug Administration (USFDA) has approved PCL, a thermoplastic polymer, for use in adhesion barriers in the human body, suture materials, and drug delivery devices. PCL has a glass transition temperature (Tg) of approximately −60°C and a melting point of around 60°C. It is a biodegradable, semicrystalline polyester that breaks down under physiological circumstances by hydrolyzing its ester bonds. The biodegradation rate of PCL is far slower than that of the majority of natural polymers, including collagen, fibrin, and gelatin [77].

3D-printed scaffolds constructed from polycaprolactone (PCL) and bioink produced from decellularized human cartilage were utilized in a study to improve mechanical stability and tissue regeneration. Similar to natural cartilage, the de-cellularization technique preserved glycosaminoglycan and total collagen while successfully eliminating cellular components. The bioink was formulated by incorporating decellularized human cartilage particles into hyaluronic acid and carboxymethyl cellulose gels, optimizing the rheological properties for 3D printing. The decellularized bioink made from human cartilage showed no cytotoxicity in *in vitro* testing, and it promoted the migration and chondrogenic differentiation of human adipose-derived stem cells. Using this bioink in conjunction with PCL, 3D-printed scaffolds were generated, and the effectiveness of the scaffolds was assessed in rabbits over the course of a year after implantation. According to the results, the scaffolds showed notable neovascularization and chondrogenesis and retained their structural integrity throughout the course of the year. In scaffolds with higher ratios and more decellularized cartilage, histological investigation showed enhanced blood vessel development [78].

The natural human meniscus, which has a zone-specific biochemical composition, was intended to be functionally and structurally mimicked by the 3D-printed meniscus scaffold. In particular, the design included a cartilaginous inner area and a fibrous outer portion. A composite material made of polycaprolactone (PCL) reinforced with nanohydroxyapatite (HA) was chosen as the base component in order to accomplish this. The selection was based on the material's mechanical characteristics, which closely resemble those of natural meniscus tissue. Two different hydrogels were used as bioinks: glycidyl methacrylate-modified silk fibroin (PVA-g-GMA/SF-g-GMA) for the inner region, which was intended to induce chondrogenesis, and gelatin methacrylate (GelMA) for the outer region, which was thought to encourage fibrogenesis. The scaffold was printed using a dual-nozzle 3D printing method. The inner area demonstrated chondrogenic properties while the outside region successfully displayed fibrogenic features, both of which successfully mirrored the zonal biochemical composition of the natural meniscus. Additionally, the mechanical characteristics of the 3D-printed PCL/HA/hydrogel scaffold were similar to those of the human meniscus, ensuring structural integrity. The scaffold's form was quite similar to that of the lateral and medial menisci [79].

In another investigation, two structurally distinct scaffolds—a PCL/45S5 Bioglass (BG) composite and a PCL/hyaluronic acid (HyA) composite—were created using 3D printing technology and assessed for their ability to promote dentin and pulp tissue regeneration, respectively. Their physicochemical analysis

demonstrated that the mechanical characteristics, surface roughness, and bioactivity of the PCL/BG scaffolds were enhanced by the presence of BG. Additionally, applying HyA to the PCL scaffold's surface significantly increased the scaffolds' hydrophilicity, which improved cell attachment. Additionally, the gene expression data demonstrated that the presence of both PCL/BG and PCL/HyA scaffolds significantly increased the expression of odontogenic markers [80].

Polyurethane (PU)

PU is a class of linearly segmented polymers made up of organic (hard segment) and oligodiol (soft segment) units joined by carbamate (urethane) bonds (–NH–(C=O)–O–). Because of their superior mechanical qualities and superior biocompatibilities, PUs—which can be either biodegradable or non-biodegradable—have found extensive usage in biomedical applications. It is distinguished by the solvent used, which is either an organic solvent-based traditional PU or a water-based PU. The latter uses water as a solvent, whereas the former uses volatile organics. The chemical composition of PUs determines their physicochemical and physicochemical characteristics, including biodegradability, PH sensitivity, and thermosensitivity [81]. Because of their superior mechanical qualities, adjustable chemical structures, and greater biocompatibilities, biodegradable PUs are currently being utilized extensively for the 3D printing of bioartificial organs [82].

In a study prior to gelation, neural stem cells (NSCs) were incorporated into the polyurethane dispersions. After that, the NSC-containing dispersions were printed and kept at 37°C. The NSCs in PU hydrogels demonstrated superior differentiation and proliferation. Furthermore, the function of the impaired nervous system may be restored by injecting NSC-rich PU hydrogels into the zebrafish embryo neural damage model. Moreover, following the implantation of the 3D-printed NSC-loaded PU structures, the function of adult zebrafish suffering from traumatic brain damage was restored [83].

In another work, a novel waterborne PU (WBPU)gel that is biodegradable and thermoresponsive was developed as a bioink. For cell reprogramming, PU hydrogel was co-extruded with human fibroblasts and FoxD3 plasmids. The outcomes demonstrated that human fibroblasts co-printed with FoxD3 in the thermoresponsive PU hydrogel could undergo reprogramming and develop into cells that resembled neural crest stem cells and had an elevated cell viability [84].

In a different study, 3D bioprinting technology was used to generate scaffolds made of functional alginate and WBPU for the regeneration of articular cartilage. Mature chondrocytes have been embedded into various alginate-WBPU inks in order to manufacture the scaffolds for 3D bioprinting. Bioinks demonstrated superior 3D printing capability, cell viability, and structural integrity, making them ideal for scaffold construction. Following 28 days of *in vitro* cartilage formation experiments, scaffolds maintained a cell population of 10^4 chondrocytes/scaffold in differentiated phenotypes and were able to synthesize up to 6 μg of glycosaminoglycans (GAG) and specialized ECM [85].

Polyvinylpyrrolidone

Poly(N-vinylpyrrolidone) (PVP), a synthetic polymer that has been around since 1938, has a distinctive ability to dissolve in water and a variety of organic solvents. Researchers have shown considerable interest in PVP for biomedical applications, attributed to its inert characteristics, stable chemical composition, low toxicity, non-irritating effects on biological systems, and overall biocompatibility. PVP has found broad application in the development of hydrogels, wound dressings, nanofibers/scaffolds, drug delivery systems, and gene therapies [86].

In a study, the physical characteristics of the bioinks were altered using an inert polyvinylpyrrolidone (PVP360, molecular weight = 360 kDa) polymer, and the impact of these qualities on printing efficiency and

cell health was examined. The findings of the experiment demonstrated that a greater viscoelasticity of the bioink aids in stabilizing droplet filaments prior to their rupture from the nozzle orifice. Since the polymer in the printed droplets gives the encapsulated cells an extra cushioning effect (greater energy dissipation) during droplet impact on the substrate surface, improves the measured average cell viability even at higher droplet impact velocity, and preserves the printed cells' ability to proliferate, additional analysis revealed that cell-laden bioinks with higher viscosity exhibited higher measured average cell viability (%) [87].

PCL and PVP were employed as matrix polymers in an investigation by Izgordu et al. Low-molecular-weight chitosan (CS), hyaluronic acid (HA), and alginic acid sodium salt (SA) were integrated independently with the polymer matrix to create the constructs. According to the findings of mechanical characterization, the printed PCL/3wt.%PVP/1wt.%CS had the maximum compressive strength, measuring around 9.51 MPa. 5.38 MPa was the difference in compressive strength between PCL/3wt.%PVP and PCL/3wt.%PVP/1wt.%CS. Mitochondrial dehydrogenase activity was used to examine the constructions' biocompatibility, and *in vitro* experiments using the mesenchymal stem cell line revealed that the PCL/3wt.%PVP/1wt.%HA composite construct had higher cell viability than the other constructs [88].

Another study used macromolecules of PVP to generate bioink. The printability of several PVP-based bioinks was assessed, and the printed cells' short- and long-term vitality was initially examined. The results showed that a bioink with a threshold Z value of ≤9.30 may print cells without causing any major problems. The survival of printed cells is dependent on the Z values of the bioinks. The cell production was then assessed for 30 min. PVP molecules were shown to reduce cell adhesion and sedimentation throughout the printing process; the 2.5% w/v PVP bioink showed the most constant cell output over a 30-min timeframe, enhancing cell survival and homogeneity throughout the bioprinting experience [89].

Poly(L-Lactic) Acid (PLA)

PLA is an aliphatic and biodegradable polyester made from lactic acid obtained from renewable sugarcane or maize starch. The cyclization and oligomerization processes combine to form PLA, or lactic acid cyclic dimer. Due to its biocompatibility and lack of toxicity or carcinogenic effects on local tissue, PLA is frequently utilized in biomedical applications [90].

A 3D printed PLA: calcium phosphate (CaP): Graphene oxide (GO) scaffold was designed in a study for bone tissue engineering purposes. Polylactic acid (PLA), CaP, and the optimized GO dose (0.10 mg mL−1) were combined to fabricate a 3D printed PLA: CaP:GO scaffold, which upon physicochemical characterization (SEM/EDS, XRD, FT-Raman, nano-indentation) and *in vivo* tests, confirmed its biocompatibility, enabling a novel approach for bone tissue-related applications [91].

In a study, mixed matrix scaffolds were created using a PLA/mesoporous bioactive glass (MBG) composite with a weight ratio of 30:70, which resembles the natural bone composition. According to the SEM study, the 3D printed PLA/MBG composite scaffolds have pores that range in size from 500 to 700 μm, indicating that they are macroporous and beneficial for bone cell proliferation. The PLA/MBG composite scaffold's good bioactivity behavior was demonstrated by the *in-vitro* bioactivity evaluation, which revealed quick apatite crystallization by achieving a Ca/P ratio of 1.66 similar to natural bone mineral during the third day after SBF treatment. Through *in-vitro* biological evaluation utilizing MG-63 osteosarcoma cells, the 3D bioprinted PLA/MBG composite scaffold shown encouraging responses in terms of cell attachment and proliferation, mineralization, and gene expression features [92].

Kolan et al. examined the survival of human adipose-derived mesenchymal stem cells (ASCs) in an alginate-gelatin (1:1) hydrogel (bioink) that is deposited in the spaces between composite filaments of PLA and borate glass. PLA + B3 glass composites were generated by adding B3 glass to PLA in two distinct weight ratios (50 and 33%). The mechanical characteristics, pH change of the surrounding fluid, and weight

loss of the 3D printed composite scaffold were all examined over time. A physical examination of the composite scaffolds revealed full glass dissolution after two weeks and enhanced mechanical qualities. To examine ASC viability, cellularized scaffolds were bioprinted in three different configurations: PLA + Bioink, PLA + Bioink, and PLA + B3 glass + Bioink. They were then grown under dynamic circumstances. With hypoxic-like circumstances and decreased viability in the bottom area to higher viability in the upper layers of the scaffold, the results showed non-uniform cell viability along the scaffold thickness [93].

Polylactic-Co-Glycolic Acid (PLGA)

PLGA is a biodegradable functional polymer organic molecule formed by the polymerization of two monomers, lactic acid (LA) and glycolic acid (GA), with excellent biocompatibility and no biotoxicity [94]. Depending on the LA:GA ratio, PLGA's molecular weight (g/mol) can range from thousands to hundreds of thousands. Because of its biodegradability, biocompatibility, broad range of erosion times, and flexible mechanical qualities, PLGA is widely employed in tissue engineering and drug administration. The FDA has authorized this polymer due to its physical strength and biocompatibility, which have led to its widespread usage in several studies [95].

In one study, a 3D printed dermal scaffold containing bioactive PLGA was designed for burn wound healing. Ring-opening metathesis polymerization (ROMP) was used to create bioactive brush copolymers with pendant side chains of PLGA and PEGylated Arg-Gly-Asp tripeptide (RGD) or HA. These copolymers demonstrated strong thermal stability when processed using melt-extrusion techniques. The 3D printed scaffolds showed high biocompatibility in both *in vivo* animal models and *in vitro* cell testing. In comparison to Biobrane, the clinical gold standard for treating second-degree burn wounds, a porcine investigation using a partial thickness burn wound model demonstrated that these PLGA scaffolds promoted re-epithelization with less inflammation [96].

Song et al. studied the impact of three-dimensional (3D) printed PLGA scaffolds mixed with Gly-Phe-Hyp-Gly-Arg (GFOGER) and bone morphogenetic protein 9 (BMP-9) on extensive bone defect recovery. PLGA scaffolds were created using the 3D printing technique, and the sample was examined using optical microscopy, SEM, XRD analysis, water absorption, compressive strength, and other techniques. This scaffold has slower rates of degradation and mechanical qualities that are acceptable. Over the course of a 12-week *in vivo* investigation, the scaffold demonstrated improved new bone mineral deposition and density following surface modification using GFOGER peptide and BMP-9. This scaffold up-regulated the expression of Runx7, OCN, COL-1, and SP7, which helped to produce the observed uniform trabeculae development and new bone regeneration, according to histological examination and Western Blot [97].

Choe et al. designed a variety of bioinks for mesenchymal stem cell (MSC) printing and osteogenic differentiation induction utilizing poly(lactic-co-glycolic acid) (PLGA) nanoparticles loaded with bone morphogenetic protein-2 (BMP-2). PLGA nanoparticles added to alginate might boost the bioink's printability and mechanical characteristics. BMP-2-loaded PLGA nanoparticles (NPBMP-2) exhibited up to two weeks of sustained BMP-2 release *in vitro*. Additional *in vitro* research revealed that, in comparison to other controls, bioinks made of alginate and NPBMP-2 markedly increased the osteogenesis of MSCs, as shown by increased calcium deposition, alkaline phosphatase activity, and osteogenic marker gene expression [98].

Polyvinyl Alcohol (PVA)

PVA, a synthetic polymer made by breaking down poly (vinyl acetate), has the repeating unit [-CH_2-CH(OH)-]n and dissolves easily in water. Because of the large number of hydroxyl (-OH) groups that are distributed throughout its backbone, it is highly water-attracting (hydrophilic) and has the ability

to create hydrogen bonds. PVA's well-known ability to form thin films is also a result of these properties. Importantly, PVA's hydroxyl groups make it simple to modify or combine with other polymers, improving its mechanical strength and flow characteristics—two crucial aspects for utilization in bioinks and 3D printing [99].

Small-diameter artificial blood vessels were developed in a study using a porous composite hydrogel of sodium alginate, gelatin, and polyvinyl alcohol (SA/Gel/PVA). Using the multiple crosslinking approach, the porous composite hydrogel ink was designed with the goal of resolving the issues of inadequate mechanical characteristics and an unsatisfactory printing effect of blood vessels with tiny diameters [100].

Polyvinyl alcohol cryogels (PVA-C) were used in an alternate study for vascular tissue engineering because of their hydrophilicity, biocompatibility, and mechanically adjustable qualities. Sub-zero extrusion-based three-dimensional (3D) bioprinting was used to manufacture multi-layered PVA-C structures, and their mechanical performance was examined. The outcomes demonstrated that a multi-layered design affects PVA-C's mechanical profile and indicated that functionally graded design techniques might improve compliance matching and replicate native blood vessel biomechanics in small-diameter vascular grafts [101].

A new 3D bioprinted construct was designed by Loukelis et al. using pre-osteoblastic cells, the synthetic polymer PVA and the natural anionic polysaccharide gellan gum (GG). Additionally, as an osteoinductive biomaterial, nano-hydroxyapatite (nHA) was added to the GG/PVA blend. The findings showed that the generated bioinks had biological responsiveness and viscoelastic characteristics that make them appropriate for bone tissue engineering applications [102].

3.2 Bioceramics

Bioceramics are a category of ceramics that emerged in the 1970s. Bioceramics offer superior biocompatibility and bioactivity potential in addition to the mechanical qualities of ceramics. Thus, these biomaterials are also utilized in the field of tissue engineering to induce osteogenesis in many dental implants, bone grafts, and scaffolds [103]. However, the brittle surface and limited elasticity of bio-ceramics restrict their application in implants. To increase their strength and flexibility, they are typically coated or mixed with other materials. Alumina, zirconia, bioactive glass, glass-ceramics, hydroxyapatite, and resorbable calcium phosphates are some of the most extensively utilized bioceramics [103,104]. High density ceramics like zirconia and alumina have excellent mechanical strength and resistance to corrosion; nevertheless, prior research indicates that zirconia is somewhat less resistant to corrosion than alumina. The two may be used as hip and knee replacement components since they are also biocompatible and bioinert. As a body implant, they can reduce negative tissue responses to ion toxicity from metallic stents or prostheses and provide structural support that prevents stress shielding.

3.2.1 Hydroxyapatite (Hap)

The chemical formula for HAp, a naturally occurring calcium phosphate-based mineral, is $Ca_{10}(PO_4)_6(OH)_2$. Its structure is comparable to that of bone mineral, a biological apatite found in the human body that accounts for between 60 and 70 percent of the dry weight of human bone tissues. Its physical and chemical characteristics are comparable to those of human bone and tooth tissues [105]. Hydroxyapatite is well-known for its capacity to repair injured cells and form connections with nearby tissues. Because of its bioactivity and bioresorbability, osteogenesis will stop when the substance eventually dissolves in the body. Therefore, scaffolds are made from hydroxyapatite-rich natural materials such as animal bones, corals, algae, shells, and fish scales [106]. HAp has great osteoinductivity and osteoconductivity, as well as outstanding biocompatibility and bioactivity, non-inflammatory and non-toxic properties. Additionally, it stimulates cell growth and proliferation and vitalizes growth factors. Thus, HAp is regarded as a very promising bone

replacement and implant material. However, HAp is not appropriate for many BTE applications due to its poor mechanical qualities, sluggish resorption and remodeling rates, and slow degradation rates *in vivo*. For this reason, HAp is typically combined with other synthetic or natural polymers to produce composite scaffolds that are more effective [107].

The investigation involved the preparation of polymer solutions based on methacrylated gelatin and methacrylated hyaluronic acid modified with HAp particles (5 weight percent) as primary human adipose-derived stem cells were encapsulated in HAp-containing gels and cultured for 28 days, the storage moduli ascended substantially to 126% ± 9.6% as compared to the value on day 1 due to the HAp's exclusive impact. The ink demonstrated outstanding printability when used as bioinks to build up pertinent geometries utilizing the cell-laden polymer solutions, and the integrity of the printed grid structure held up during a 28-day culture period. As shown by rheological measurements and bone component staining, the results showed that HAp-containing bioinks and hydrogels based on methacrylated gelatin and hyaluronic acid are both highly appropriate for the development of pertinent three-dimensional geometries with microextrusion bioprinting and have a notable positive impact on bone matrix development and remodeling in the hydrogels [108].

In another investigation, two bioinspired nanohydroxyapatite (nHA)s, differing in their chemical compositions, crystallinity, and structures, were produced and analyzed: one is a more crystalline, needle-shaped Mg_{2+}-doped nHA (N-HA), while the other is a more amorphous, rounded Mg^{2+}- and CO_3^{2-}-doped nHA (R-HA). To explore how various compositions and structures of these nanoparticles influence the bioprinting of human bone marrow stromal cells (hBMSCs), gelatin and gelatin methacryloyl (GelMA) were chosen as the backbone for the bioink. Both nHAs demonstrated substantial cell viability, with N-HA exhibiting a large increase in metabolic activity under non-osteogenic conditions and R-HA exhibiting a considerable increase with osteogenic stimulation. These results emphasize the significance of both chemistry and morphology in bioink performance by indicating that the two nHAs interact with their surroundings in distinct ways. Osteogenic differentiation further demonstrated how nHAs' physicochemical characteristics affect osteogenic markers at the RNA and protein levels [109].

Using silk-hydroxyapatite bone cements with osteoinductive, proangiogenic, and neurotrophic growth factors or morphogens for faster bone formation, functionalized 3D-printed scaffolds for bone regeneration were created in another study. Building on the understanding that the osteoinductive factor Bone Morphogenetic Protein-2 (BMP2) can also favorably impact vascularization, Vascular Endothelial Growth Factor (VEGF) can affect osteoblastic differentiation, and Neural Growth Factor (NGF)-mediated signaling can affect bone regeneration, 3D printing was used to create macroporous scaffolds with controlled geometries and architectures that support osseointegration. The materials were osteoconductive, cytocompatible, and preserved the action of the morphogens and cytokines, and the scaffolds had mechanical qualities appropriate for bone. Based on the overexpression of genes linked to osteoblastic differentiation, synergistic effects of BMP-2, VEGF, and NGF were found in terms of osteoblastic differentiation *in vitro* [110].

3.2.2 Tricalcium Phosphate

Numerous ceramics based on calcium phosphate (CaP), including hydroxyapatite (HA), biphasic calcium phosphate (BCP), calcium polyphosphate (CPP), and β-tricalcium phosphate (β-TCP), have exceptional osteoinductive and osteoconductive qualities. Although β-TCP and hydroxyapatite (HA), the mineral component of natural bone tissue, have molecular similarities, β-TCP degrades more quickly because of its lower Ca/P ratio. When processed into different porous shapes, β-TCP, a biocompatible ceramic, offers an environment that is conducive to cell adhesion and growth. However, ceramics are problematic to utilize in load-bearing body areas because of their high brittleness and poor strength [111].

Melo et al. coated 3D-printed β-TCP scaffolds with bioactive glasses, 45S5 ($45SiO_2$–$24.5Na_2O$–$24.5CaO$–$6P_2O_5$, wt.%) and 58S ($58SiO_2$–$33CaO$–$9P_2O_5$, wt.%), utilizing sol-gel solutions using a vacuum impregnation approach. The β-TCP ink displayed pseudoplastic behavior, which facilitates 3D printing. With well-aligned filaments and little collapse of the bottom layers during sintering, the resultant scaffolds showed excellent reliability to the designed model. An apatite mineralization experiment in simulated bodily fluid was used to validate bioactivity. It showed that both coated scaffolds precipitated hydroxyapatite, albeit in different morphologies [112].

β-TCP scaffolds with different amounts of multi-walled carbon nanotubes (MWCNT) (0.25–1.00 wt%) were designed in a study. The results show that adding MWCNTs improved the viscosity of β-TCP suspensions in a concentration-dependent manner. The addition of MWCNT decreased the *in vitro* degradation of β-TCP and altered compressive strength. Furthermore, the results showed that the scaffold enhanced the expression levels of the genes for alkaline phosphatase, osteopontin, and osteocalcin in adipose-derived stem cells; however, MWCNT produced greater levels of gene expression [113].

In another study, cationic functional molecules were added to hydroxyapatite nanoparticles. In the 3D-printed tricalcium phosphate/hydroxyapatite (TCP/HA) scaffold, 3-aminopropyltriethoxysilane (HA-NPs-APTES) containing microRNA-302a-3p (miR) can promote the repair of the critical-sized bone defect. Two techniques were used to modify 3D-printed TCP/HA with HA-NPs-APTES (M1, M2). The M1 and M2 scaffolds both have cell adhesion on their surface and were biocompatible. Following effective delivery, the M2 scaffold demonstrated a significant increase in miR, which led to the overexpression of RUNX2 mRNA and the downregulation of its target mRNA, COUP-TFII. At all-time points, the calvarium defect with M2 scaffold also had much greater BV/TV and more filled gaps. New bone grew at the middle of the HA-NPs-APTES-miR scaffold earlier than controls, according to histomorphometry. HA-NPs-APTES-modified TCP/HA scaffold improved bone regeneration and made miR distribution easier [114].

3.2.3 Bioactive Glass

In 1971, Hench et al. discovered 45S5 bioactive glass (45S5 Bioglass®), a silicate glass with 45% silica (SiO_2), 24.5% calcium oxide (CaO), 24.5% sodium oxide (Na_2O), and 6% phosphorous pentoxide (P_2O_5), which paved the way for the field of bioactive materials. “Bioactive” in this instance describes “a material that elicits a specific biological response at the material surface which results in the formation of a bond between the tissues and the materials”. Bioactive materials are designed to modify the extracellular matrix in a regulated way and interact with the biological environment to provide the desired therapeutic effect. Bioactive materials are preferred for BTE scaffolds for the repair or replacement of bones, joints, and teeth. Bioactive materials, such as bioactive glasses (BGs) and bioactive ceramics, modify their surfaces dynamically in response to biological fluids. The creation of a highly reactive hydroxycarbonate apatite (HCA) layer offers a bonding contact with both bone and soft tissues [115]. BG utilized in bone tissue engineering is often categorized as silicate-, phosphate-, and borate-based BG, based on the forming units of the glass network. Although bulk BG may be used in bulk form to repair bone defects, BG/polymer composites are a more practical option because of their higher ductility and plasticity [116].

In a research, silicate-based, three-dimensional bioactive glass scaffolds were constructed employing novel sol-gel ink-based robocasting, and their structural and morphological properties were investigated. Furthermore, under static conditions, their *in vitro* bioactivity was examined in phosphate-buffered saline at 37°C and simulated body fluids. In contrast to the colloidal-based robocasting approach that uses bioactive glass particles, the results show that the patterned, multilayered, macroporous bioactive glass scaffolds can be successfully formed. Additionally, the structures prepared in this manner can be manufactured in

considerably finer filament dimensions. Additionally, it was demonstrated that the bioactive glass scaffolds, which were maintained in physiological fluids, developed hydroxyapatite on their surface [117].

In another paper, two-photon lithography (TPL) is employed for the first time to form BG with single-micron features. A composite comprising BG nanoparticles is constructed with TPL and thermally treated to yield glass scaffolds. The glass utilized in a study showed cytocompatibility with human mesenchymal stromal cells (MSCs) and *in vitro* bioactivity in simulated bodily fluid, which qualified it as a material for tissue engineering [118].

In another study, nanocomposites were made using mesoporous bioactive glasses (MBGs) in the ternary SiO_2, CaO, and P_2O_5 system doped with metallic silver nanoparticles (AgNPs) that were homogeneously inserted in the MBG matrix. Three-dimensional mesoporous bioactive glass scaffolds with silver were developed, displaying mesopores, macropores, and ultrapores that are evenly linked. The biological characteristics of Ag/MBG nanocomposites were assessed using MC3T3-E1 preosteoblastic cell culture tests and bacterial (E. coli and S. aureus) assays. The findings demonstrated that while preosteoblastic proliferation declined with increasing silver concentration, MC3T3-E1 cell shape remained unaffected. According to antimicrobial experiments, the higher concentration of AgNPs in the MBG matrices was positively correlated with the suppression of bacterial growth and the breakdown of biofilms. Moreover, *in vitro* co-culture of S. aureus bacteria with MC3T3-E1 cells demonstrated that AgNPs had a minor impact on cell proliferation measures and that their presence was essential for antibacterial action [119].

3.3 Metals

Because of their superior mechanical qualities and structural stability, metals—the first materials to be employed as orthopedic devices—have proven to be appealing biomaterials for bone implants. However, employing metal as a scaffold has several drawbacks. A metal implant, for example, has a greater Young's modulus than natural bone, which may result in stress shielding, which is a reduction of bone as a result of the implant removing stress from the bone. Another disadvantage of using metal as a scaffold is its low degradability, which might eventually prevent the host cells from forming new bone tissues and result in long-term concerns, including inflammation and corrosion. Numerous approaches were proposed to address this, including boosting porosity and mixing metal with other substances that can offset its disadvantages [120].

Bone scaffolds have been made using iron (Fe) and magnesium (Mg)-based metals, including pure Fe, Mg-RE (rare earth) alloys, Mg-Ca, Fe-Mn alloys, and Fe foam. Compared to magnesium (41GPa) and its alloys (44GPa) and 316L stainless steel (190GPa), iron has a greater elastic modulus (211GPa) [121]. Ti, Ti alloys, Mg, Fe, 316L stainless steel, and NiTi are the metal scaffolds constructed primarily using AM. Due to its inexpensive cost and comparable elastic modulus to human bone, Ti–6Al–4V (Ti alloy) is a preferred choice [122].

For metallic scaffolds, magnesium and its alloys work well as well. They are biodegradable in biological fluids, have mechanical qualities comparable to those of human bone, and have an ionic composition that is compatible with the body's physiological systems. Because magnesium alloys have a lower elastic modulus than titanium alloys, they can lessen the stress-shielding effect, which is the reduction of bone density brought on by the removal of normal stress from the bone as a result of the presence of an implant, which causes the implant to loosen. Nevertheless, their fast rate of corrosion results in the quick release of breakdown products into the body [122].

Due to its robust mechanical qualities, superior biocompatibility with living tissues, and exceptional longevity, titanium and its alloys have been among the most widely used metal-based bone implants since they were first used in surgeries in the 1950s. Ti is readily formed and adjusted to imitate the mechanical

characteristics of bone, providing an osteogenic environment for cells [123]. However, Ti cannot be replaced by newly developed bone since it is not osteoconductive and biodegradable under normal physiological circumstances. Furthermore, bulk Ti implants may result in stress shielding because of the significantly larger Young's modulus of Ti compared to cortical bone [124]. Numerous strategies including coating, surface treatment, and structural modification, were proposed to address its shortcomings [120].

A variety of coating techniques were proposed for Ti, including coating with antimicrobial substances to avoid implant-induced inflammation [125] and coating with osteogenic agents, such as HAP or silica nanoparticles to encourage bone growth [126,127]. Kapat et al. employed powder metallurgy to create Ti_6Al_4V with various pore sizes and porosities, and then assessed the pore distribution, mechanical characteristics, surface roughness, contact angle, and protein adsorption capacity. The optimum effect on cell distribution and differentiation was established by further *in vitro* and *in vivo* studies [128]. High biocompatibility and considerable flexibility for bone scaffolding have been demonstrated by nitinol (NiTi), a titanium-nickel metal alloy that has also been utilized for nail production and as a spine separator in the treatment of scoliosis. It is widely used in orthopedic implants, such as spinal rods, arc nails, artificial ribs, arched connections, patellar concentrators, three-dimensional memory alloy fixation systems, and interbody fusion devices, because of its beneficial shape memory effect and superelasticity [129].

Since SS has a high chromium content (12%) and is biocompatible and corrosion resistant, it is one of the common metal biomaterials used in orthopedic implants. Because of its desirable mechanical qualities, stainless steel may be used as a sturdy scaffold in a variety of load-bearing shapes, including plates, rods, and screws. However, SS requires additional improvements, such as surface modification, coating, and material combination, to promote bone regeneration without significantly altering its advantageous qualities [130,131].

Cobalt, a crucial component of cobalamin, promotes angiogenesis and red blood cell formation by activating hypoxia-inducible factor 1 (HIF-1), which in turn speeds up bone repair. More precisely, cobalt is known to cause hypoxia, which activates HIF-1 and promotes cellular processes that promote regeneration [132]. Furthermore, the production of collagen matrix for bone regeneration is significantly impacted by cobalt. Because of its mechanical strength and *in vivo* corrosion resistance, cobalt chromium is one of the most commonly utilized alloys in the area of regenerative medicine [133].

In a study, calcium/cobalt alginate beads were utilized to encapsulate human adipose-derived mesenchymal stem cells. Instead of depending on expensive growth factors like transforming growth factor betas or bone morphogenetic proteins to facilitate the differentiation of human adipose-derived mesenchymal stem cells into chondrocytes that produce cartilage, these advanced scaffolds for promoting chondrogenesis utilize the combined effects of the alginate matrix and Co^{+2} ions [134].

In an alternate investigation, new scaffolds made of porous PVA polymer and bioactive glasses (BG) with cobalt were developed by combining the non-toxicity, non-carcinogenicity, and processability of PVA with the osteogenic and bioactive qualities of BG and the angiogenic effect of Co using the sol-gel and foaming processing methods. This resulted in a new scaffold with angiogenic qualities. Co-incorporated samples had favorable pore sizes and high porosity. In tissue engineering applications, PVA–BG hybrid scaffolds with Co demonstrated an ionic release rate within the therapeutic range and show potential for angiogenesis [135].

3.4 Carbon Based Nanomaterials

Since carbon and carbon-based materials have unique mechanical, electrical, thermal, tribological, and biological properties that enable high-performance applications in every conceivable industrial field—from biotechnology to aerospace, from energy to electronics—they are frequently positioned as the materials of

the future. Typically, a single kind of carbon material has been used with varying degrees of effectiveness to restore a single tissue. Remarkably, recent breakthroughs in the synthesis, processing, and use of carbon-based materials, such as the discovery of carbon nanotubes, fullerenes, and graphene, have broadened the scope of this material family and paved the way for the creation of cutting-edge tissue engineering and biomedical devices. With their exceptional qualities and enormous potential, every class of carbon-based nanomaterials, including 3D graphite, 2D graphene, 1D carbon nano-tubes (CNTs), 0D carbon dots (C-dots), fullerene, and nanodiamonds (NDs), has captivated the materials industry [136].

Due to their chemical stability, mechanical strength, biological compatibility, and cost effectiveness, carbon-based materials have also gained interest as BTE scaffold materials in this aspect. Significant progress has been made in their applications in the context of BTE in recent decades, particularly as the 21st century has dawned [137].

3.4.1 Carbon Nanotubes Composite Materials as Scaffolds

Carbon nanotubes (CNTs) are allotropic, cylindrical nano-structured carbon. Although several additional forms of carbon nanotubes and their biocompatibility have been documented, CNTs are typically classified as single-wall carbon nanotubes (SWCNTs) or multiple walls carbon nanotubes (MWCNTs). SWCNTs tend to be curved rather than straight, with diameters that are usually between 1 and 2 nm, and are generally thinner than MWCNTs. The outer diameter of MWCNTs varies from 2 to 30 nm and is dependent on the number of layers. Although it can vary from 1 μm to a few centimeters, the length is usually in the micrometer range. Because of their distinctive structural, electrical, mechanical, electromechanical, and chemical characteristics, CNTs have been extensively studied for their potential use in regenerative medicine [138].

In a study, scaffolds made of CNT-reinforced 3D-printed polycaprolactone/β-tricalcium phosphate were developed and evaluated for their potential use in bone tissue engineering. In comparison to the polycaprolactone/β-tricalcium phosphate scaffold, the incorporation of CNTs significantly enhanced the mechanical properties, strength, and compressive modulus. Each scaffold exhibited a wide range of pore sizes (50–500 μm) and demonstrated high porosity of more than 70%. The scaffolds demonstrated remarkable biocompatibility, exhibiting hemolysis rates of less than 5% and outstanding cell viability [139].

In another work, innovative porous scaffolds were constructed by integrating varying concentrations of functionalized carbon nanotubes (fCNTs) into a matrix of hydroxyapatite (HAp) and silk fibroin (SF) and freeze-drying. The findings showed that the inclusion of fCNTs enhanced the proportion of SF's β-sheet structure and promoted the *in-situ* development of HAp inside the scaffold. According to an evaluation of the scaffold's properties, the addition of fCNTs considerably increased the compressive strength while reducing porosity and pore size. An increase in fCNT concentration is associated with an approximate decline in swelling and degradation rate, according to research on scaffold behavior in aqueous environments. All scaffolds, however, demonstrated a controlled and gradual release profile, underscoring their stability in maintaining fCNT release throughout time, regardless of the fluctuating fCNT levels. According to biological research, adding fCNTs up to 5 weight percent had no negative effects on cell adhesion or survival. The integration of fCNTs showed synergistic impacts on the scaffolds' mechanical, biological, and physical characteristics [140].

Zhao et al. used carboxylated MWCNTs and bacterial cellulose (BC) to create composites with gradients of 0, 0.25, 0.5, and 1 wt%. The most suitable filler for polycaprolactone (PCL) was determined to be 1 weight percent MWCNT@BC based on its physicochemical characteristics, bioactivity, and osteogenic performance. With a compressive strength of 85.99 ± 10.03 MPa, the scaffold demonstrated improved mechanical characteristics and an appropriate scaffold design. Cellular tests showed that the scaffold has

high osteoinductive performance, cell adhesion qualities, and biocompatibility. This was supported by a rat mandibular defect model that demonstrated outstanding biocompatibility and mandibular healing capabilities *in vivo* [141].

3.4.2 Graphene Based Composite Materials as Scaffolds

Graphene is a two-dimensional honeycomb structure made up of carbon atoms. The graphene family includes several derivatives such as graphene oxide (GO), reduced graphene oxide (RGO), graphene quantum dots (GQDs), graphene nanosheets, monolayer graphene, and few-layer graphene.

Graphene's high aspect ratio, mechanical qualities, and electrical conductivity have made it appealing in a variety of applications. Graphene, Graphene based materials and composites are widely employed for significant biotechnological and biomedical applications, and they are also becoming stars in scientific domains other than biology and medicine. Numerous instances have been studied in recent years, and nearly all graphene derivatives and composites are being employed and tailored to provide unique delivery carriers for drug delivery, gene therapy, and theranostics [142].

In one study, graphene and graphene quantum dots (GQD) were integrated into PCL scaffolds and compared and assessed from mechanical, biological, thermal, and surface aspects. The mechanical and biological performance of PCL scaffolds was shown to be greatly enhanced by the inclusion of both materials at a weight percentage of less than 5%. In comparison to PCL/G scaffolds, PCL/GQD scaffolds demonstrated superior compressive strength under 3%wt. while retaining the same degree of biological performance [143].

Another investigation investigated the potential combination of an organic material (collagen) and an inorganic (nano)material (GO) as components of a bioink for vascular graft bioprinting. When compared to the control formulation, the collagen and GO-modified bioink showed better mechanical and viscoelastic qualities. Furthermore, the bioink exhibited complete *in vitro* biocompatibility and no harmful effects. Coculturing human muscle cells and endothelial cells (C2C12) revealed promise for vascular graft applications [144].

In another research, PCL/GO scaffolds were generated utilizing 3D bioprinting technology for meniscus cartilage repair. GO was added to PCL scaffolds to improve their mechanical, thermal, rheological, and bioactivity characteristics. According to rheological studies, GO considerably increased the yield shear and storage modulus, indicating greater elasticity and flow resistance. According to mechanical tests, scaffolds closely resembled the mechanical behavior of the native meniscus in terms of balance and ultimate tensile strength. While DSC research showed enhanced thermal stability with higher melting temperatures, FTIR analysis verified that GO was successfully integrated into the PCL matrix without compromising its chemical integrity. A roughened appearance of the surface that promotes cellular adhesion and proliferation was shown by SEM examination. DAPI-stained fluorescence microscopy on PCL/GO scaffolds demonstrated consistent nuclear distribution and improved cell adhesion. Cytotoxicity testing verified the PCL/GO scaffolds' biocompatibility with fibroblast cells, while antibacterial assays showed greater inhibition zones against E. coli and S. aureus [145].

4 Trade-Offs between Biomaterials for 3D Printing

Despite the remarkable potential of 3D bioprinting, the achievement of fully functional bio-printed tissues and organs is still reliant on the progress of advanced bioinks. Without the right bioink formulations, issues such as inadequate mechanical stability, insufficient biological interactions, and diminished cell viability obstruct the successful conversion of bio-printed constructs into clinically relevant applications. Biomaterials utilized in tissue engineering must exhibit biocompatibility to prevent immune responses and enhance interactions between cells and materials. This necessitates the elimination of toxic or inflammatory

reactions, alongside the capability to foster cell adhesion and proliferation. The mechanical characteristics of biomaterials ought to closely resemble those of the native tissue to ensure sufficient support and uphold tissue integrity. Considerations such as stiffness, elasticity, and tensile strength are essential during the selection of materials. Additionally, biomaterial scaffolds should possess a porous interconnected structure to promote cell infiltration, nutrient diffusion, and waste elimination. The appropriate size and distribution of pores are vital for facilitating cell migration and tissue regeneration. As a result, significant research efforts are concentrated on enhancing bioink characteristics to find a balance between mechanical durability and biological efficacy, ensuring that engineered tissues demonstrate the required features for long-term viability and integration [146].

Biomaterials can be engineered to gradually degrade, facilitating the formation of new tissue while preventing complications associated with long-term implants. The rate of degradation must be customized to align with the rate of tissue regeneration, thereby providing adequate mechanical support throughout the healing process. Natural biomaterials, including collagen, fibrin, and hyaluronic acid, demonstrate outstanding biocompatibility and bioactivity. They can originate from a variety of sources, encompassing both animals and plants, and can serve to provide structural support, enhance cell adhesion, and aid in tissue remodeling. Synthetic biomaterials, including polyesters (such as polyglycolic acid and polylactic acid) as well as polycaprolactone, present a range of mechanical properties, degradation kinetics, and fabrication methods. They can be meticulously designed to fulfill specific requirements in tissue engineering. Composite biomaterials integrate the benefits of both natural and synthetic materials. For instance, hydroxyapatite (HA)-based composites replicate the mineral composition of bone, offering both mechanical support and osteoconductive characteristics. These biomaterials can be adapted to align with the properties of various tissues [147–150].

Frequently, hybrid bioinks that integrate both natural and synthetic elements are created to establish an ideal equilibrium between biocompatibility and mechanical strength. Additionally, the addition of bioactive substances, including growth factors, cytokines, cell adhesion molecules, and signaling peptides, significantly improves the biological efficacy of the bioinks, encouraging tissue-specific reactions and aiding in the differentiation of cells into functional tissue structure. Through meticulous engineering of the relationship between rheological properties and biological compatibility, researchers aspire to formulate next-generation bioinks that can mimic native tissue environments, thereby facilitating progress in tissue engineering, regenerative medicine, and the fabrication of personalized organs [151–153].

A major obstacle in the advancement of bioink technology is the fundamental trade-off between rheological characteristics and biological performance. Enhancing one aspect frequently detracts from the other. For example, raising the polymer concentration to improve the viscosity and mechanical integrity of the bioink can adversely affect cell viability or the diffusion of nutrients. Likewise, the addition of specific bioactive compounds may modify the rheological properties of the bioink, complicating the printing process. This trade-off demands a thoughtful and iterative strategy in the design of bioinks, where the particular needs of the target tissue and its application are taken into consideration. Researchers are examining a range of strategies to tackle this issue, including the implementation of composite bioinks that integrate multiple materials to produce a synergistic effect, along with the creation of stimuli-responsive bioinks that can be calibrated to alter their characteristics in response to external stimuli [147,154,155].

5 Technological Aspects for 3D Printing of Biological Matters

5.1 Data Processing

3D bioprinting begins with a computer-assisted design, which builds a specified 3D biological model. To start, a computerized three-dimensional model of the tissue defect can be made using imaging modalities

including CT, MRI, and ultrasound. The scaffold's surface and internal architecture, including pore diameters and porosity, may be integrated into the 3D model of the tissue defect using computer-aided design. A variety of materials, cell types, and bioactive chemicals can be employed to create a bioink for printing, depending on the needs, location, and kind of defect. After being transformed into a standard tessellation language file, the 3D model is stored in a file format like G-code. The printer could readily follow the file format and decipher the biological components' layer-by-layer depositions. The produced cell-laden structures are then either directly implanted into the patient or cultured in a cell culture [156,157].

5.2 3D Bioprinting Techniques

As seen in Fig. 2, the 3D bioprinting process may be categorized into four primary classes. Today, the healthcare industry and the manufacturing of medical materials have undergone significant change as an outcome of the rapid advancement of 3D bioprinting in the medical field. Complex organ and tissue structures have been constructed by this method. 3D bioprinting is divided into many categories according to its working principle. These methods can be employed separately or in a combined approach to achieve favorable tissue fabrication.

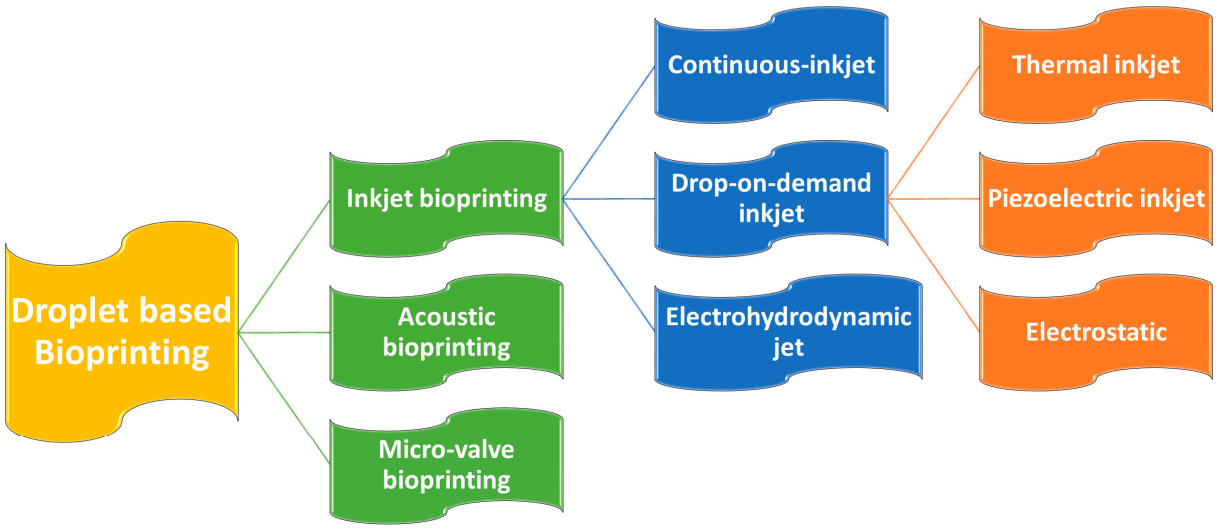

Figure 2: Classification of Droplet based bioprinting techniques.

5.2.1 Droplet Based 3D Bioprinting

Droplet-based 3D bioprinting has a number of distinct benefits over other printing methods for constructing intricate 3D structures. (i) its flexibility and superior control over small-volume droplets at precise locations, even on curved surfaces; (ii) the droplet formation mechanism permits a high-resolution, non-contact printing technique of intricate designs and structures; and (iii) its biocompatibility affirms the activity of the encapsulated particles [158].

For high-precision drug delivery and customized therapy, drop-let-based 3D bioprinting techniques may be used to create delicate constructions with a controlled drug dosage utilizing cell-free bioinks. On the other hand, time-consuming animal experiments and basic 2D cell culture models are replaced with tissue constructions with cells encapsulated in cell-laden bioinks, which offer a more effective and productive approach for *in vitro* drug screening. All things considered, droplet-based 3D bioprinting can produce complex and diverse 3D structures with great efficiency while preserving the ability of cells or medications to function effectively [159].

In summary, droplet-based 3D bioprinting provides significant benefits, including (i) the ability to accurately modulate drug dosage and formulation within small volume droplets for targeted drug delivery; and (ii) facilitating the creation of biomimetic heterogeneous tissues and organs, suitable for drug screening while minimizing material, time, and laboratory space usage, highlighting its immense potential for high throughput drug screening [158,159].

Droplets are formed by physically manipulating a bioink solution in inkjet bioprinting. It incorporates the fluid mechanics of the bioink solution, air pressure, and gravity to propel droplets onto a receiving platform [158]. Piezoelectric/thermal force works in piezoelectric/thermal ink jetting to eject droplets by creating pressure pulses in the nozzle. On the other hand, electrohydrodynamic jetting uses an electric voltage to create droplets, while acoustic wave jetting uses the acoustic radiation force produced by an acoustic actuator [160,161]. Drop-on-demand inkjet bioprinting works by automatically delivering a regulated volume of bioinks, generally including cells, in the form of droplets to predetermined sites [162]. In Continuous inkjet bioprinting, the bioink solution is pressured through a nozzle, which then divides into a flow of droplets due to the effect of Rayleigh-Plateau instability [163]. Micro-valve bioprinting uses an electromechanical valve to generate droplets. The bioink in the fluid chamber is pressurized (back pressure) and the nozzle orifice is gated by a micro-valve [164].

5.2.2 Vat Polymerization

The vat polymerization method is founded on polymeric solutions using a laser-based solidification approach. Thus far, the primary types of vat polymerization methods that have been presented are digital light processing (DLP), and stereolithography (SLA).

Stereolithography is a process of sculpting things in which a photopolymerizable material is exposed to UV light selectively, and the material cures as a result of the light exposure [165]. The laser beam provides the conditions required to start the photopolymerization process [166] and will likely assure the reaction of the photoinitiator in the resin or form a bond with the existing monomers. The SLA method uses low-power UV irradiation for photopolymerization, which is typically produced by a He-Cd/Nd: YVO4 laser or, in previous systems, a He-Cd laser [165]. The process of photo-induced polymerization is a chain reaction where hundreds of monomer/oligomer units are incorporated after a single photon produces the starting species. Thus, liquid monomers are transformed into solid polymers in a matter of seconds during photopolymerization [166].

Whereas digital light processing uses a digital light projector as a light source, stereolithography uses a UV laser beam to harden materials. Incoming UV light is reflected by a micromirror device that uses sequentially loaded user-defined patterns to switch on and off mirrors [167]. Photocurable bioinks are selectively solidified in this layer-by-layer procedure that is managed by a movable stage along the z-axis. In order to save printing time, whole layers may be created concurrently in a single exposure phase. Additionally, the nozzle-free approach prevents clogging and extreme shear stress on cells [168].

The potential for cytotoxic effects from photoinitiations and UV light exposure limits both digital light processing and stereolithography [169]. Furthermore, the necessity for easy crosslinking via light irradiation to enable the uncured bioink to interface with the cured layers restricts the spectrum of bioinks that may be utilized in stereolithography and digital light processing bioprinting [170].

5.2.3 Extrusion-Based Bioprinting

Extrusion-based tissue scaffold bioprinting is a method that enables the precise deposition of filaments, fibers, or droplets composed of biomaterials and cells, thereby facilitating the construction of tissue scaffolds in a controlled, layer-by-layer manner. This bioprinting approach integrates a fluid-dispensing head with

an automated robotic system [171]. Extrusion-based bioprinting techniques can be categorized into three distinct types based on their deposition mechanisms: pneumatic, piston, and screw-based bioprinting. Among these, pneumatic-based bioprinting is a widely employed and straightforward method that employs compressed air to propel biomaterials or cells from a syringe and nozzle, allowing for precise control over the volumetric flow rate. A linear moving piston or a rotating screw-driven arrangement physically pushes biomaterial/cell solutions in piston- or screw-based bioprinting devices. Large deposition forces are available for both printing methods, allowing for solution volume control. Consequently, a greater pressure differential between the syringe inlet and the nozzle outlet is advantageous for the printing of suspensions with higher viscosities [168,171].

Extrusion-based bioprinting (EBB) has emerged as the predominant technique in the field of bioprinting [172]. Its widespread adoption can be attributed to its ability to print hydrogels with a broad range of viscosities (from 30 mPa·s to over 6×10^7 mPa·s) and to produce large-scale three-dimensional models (on the centimeter scale) with high cellular densities (exceeding 10^8 cells/mL) [173]. Nevertheless, the resolution of this process is limited, with the minimum feature sizes achievable ranging from 200 to 1000 μm, which poses challenges in replicating the intricate structures characteristic of biological tissues [174]. Furthermore, there exists a trade-off between optimizing printing performance and ensuring high cell viability. For example, certain biomaterials (such as Pluronic, PEG, and alginate) that exhibit advantageous rheological and mechanical properties may create a suboptimal environment for cellular health. Conversely, other natural biomaterials (including collagen, gelatin, chitosan, fibrin, and decellularized extracellular matrix (dECM) that possess beneficial biological properties often demonstrate inadequate rheological and mechanical performance [175]. This dichotomy in material properties can be addressed through various strategies, including modifications to the printing environment, optimization of bioink formulations, exploration of crosslinking mechanisms, and the incorporation of sacrificial materials to enhance the mechanical and temporal stability of the bioprinted constructs [173–175].

5.2.4 Laser Assisted Bioprinting

The process of laser-assisted bioprinting of biological materials, specifically living cells, is fundamentally grounded in the laser-induced forward transfer (LIFT) technique. This method employs a pulsed laser to facilitate the transfer of material from a source film. Various adaptations of the LIFT technique have been developed to enable the printing of living cells [176]. Cells produced through this technique, when contrasted with those generated via extrusion-based methods, undergo reduced mechanical stress, resulting in enhanced viability. Nevertheless, the operational speed of this method is comparatively slower than that of extrusion-based techniques. Conversely, laser-based bioprinting facilitates the printing of hydrogels with high viscosity, exceeding the viscosity threshold applicable to droplet-based bioprinting processes [177].

The system is composed of three primary components: a pulsed laser source, a ribbon, and a receiving substrate. Nanosecond lasers emitting ultraviolet wavelengths, such as excimer lasers operating at 193 nm and 248 nm, as well as near-ultraviolet wavelengths like 1064 nm, are commonly employed as energy sources to achieve pulse energy deposition ranging from 1 to 20 μJ per pulse [178].

In a standard Laser-Induced Forward Transfer (LIFT) setup, the cell transfer module includes a ribbon and a substrate, which are typically designed as disks and made from transparent materials, such as glass or quartz. The ribbon is positioned above the substrate with a minimal gap, generally between 100 and 500 μm [179]. Transparent glass, a thin coating of metal that absorbs laser light, such titanium or gold, and a suspended layer of bioink made of cells, hydrogels, and bioactive ingredients make up the ribbon, which is a multilayer component [180].

The laser generator emits the laser beam, and after it passes through the transparent supporting structure, the mirrors and lenses alter the laser path such that the laser reaches and focuses on the upper surface of the sacrificial layer or bioink layer [179]. Galvanometric mirrors serve a critical function in directing the laser beam onto the ribbon, facilitating an increased manufacturing speed. Nonetheless, the implementation of a refractive lens is necessary to rectify the incidence angle of the laser beam on the ribbon [181].

When the laser beam is pulsed for a predetermined duration and focused on the ribbon, the metal layer situated atop the hydrogel undergoes vaporization, resulting in the formation of a high-pressure bubble that propels droplets of bioink onto the receiving substrate [178,179]. Following their transit through the interstitial space between the ribbon and the substrate, a small quantity of bioink is deposited onto the substrate, wherein the cells or other biomaterials contained within the bioink are printed. By systematically repeating these four steps—printing in various locations, droplet by droplet, and layer by layer—the intended biological structure is ultimately constructed.

6 Rheological and Structural Properties of Bioink for 3D Bioprinting

Rheology is the study of the deformation and flow behavior of materials when subjected to applied forces. The rheological characteristics of a bioink are crucial in shaping its performance throughout the bioprinting process, directly affecting its printability, structural stability, and the overall effectiveness of tissue creation. Important rheological factors—including viscosity, shear-thinning properties, and gelation rates—need to be meticulously adjusted to guarantee that the bioink can be accurately extruded, retain its form after printing, and offer a stable environment for the encapsulated cells [182].

6.1 Viscosity

Viscosity refers to a fluid's resistance to flow when subjected to applied stress and significantly impacts both the accuracy of printing and the efficiency of cell encapsulation processes. Typically, elevated viscosity levels enhance printing fidelity. Nonetheless, increased viscosity also induces greater shear stress, which may adversely affect the viability of cells suspended within the bioink. The primary determinants of polymer solution viscosity are molecular weight and concentration [183].

For example, Newtonian fluids exhibit a constant viscosity that remains unaffected by variations in shear rate. In contrast, non-Newtonian bioinks demonstrate viscosity changes that are contingent upon the applied shear conditions. Therefore, the optimization of viscosity in bioink formulations necessitates a careful balance between ensuring processability during extrusion through printing nozzles and maintaining structural integrity post-extrusion [184].

6.2 Shear Thinning

Shear-thinning is the predominant kind of time-independent non-Newtonian fluid behavior, characterized by a reduction in viscosity with increasing shear speeds. Polymer melts, polymer solutions over a threshold concentration, partly cross-linked hydrogels, colloidal suspensions, and other materials commonly used in extrusion printing usually display this feature [185].

This phenomenon is especially beneficial in bioink applications, as it enables the material to flow smoothly through printing nozzles under conditions of high shear, while preserving its structural integrity at low shear rates after deposition. The underlying mechanism responsible for this behavior involves the structural reconfiguration of polymeric networks, wherein chain entanglements and molecular interactions are disrupted by shear stress, thereby decreasing flow resistance. Materials characterized by significant

shear-thinning behavior exhibit improved printability and maintain cell viability by minimizing mechanical stress throughout the processing stage [185,186].

6.3 Viscoelasticity (G′/G″) and Yield Stress

Viscoelastic properties describe materials that concurrently demonstrate both viscous and elastic responses when subjected to deformation, reflecting the dualistic behavior of bioinks under dynamic conditions [185,186]. This behavior can be explained using two parameters: the storage (or elastic) modulus G′ and the loss (or viscous) modulus G″. The storage modulus G′ serves as a measure of the energy stored elastically during deformation, which is therefore associated with the preservation of elastic shape. The loss modulus G″ serves to measure the energy dissipated by the material, linking it to viscous flow. The viscoelastic characteristics can be assessed through oscillatory rheology, unlike viscosity, which is evaluated during rotation. The storage modulus (G′) and the loss modulus (G″) are generally measured as a function of both the frequency and amplitude of the oscillation [187].

In addition to storage modulus, the concept of shape retention can also be articulated through the yield point. This point signifies the minimum stress level necessary to commence material flow, marking the transition between solid-like and liquid-like characteristics. In bioink systems, the yield stress is crucial as it dictates the material's capacity to uphold structural integrity against gravitational forces and to support overhanging features throughout the layer-by-layer construction process. Generally, materials that display yield stress behavior maintain their dimensional stability until the applied stress surpasses the critical threshold, beyond which they behave as viscous liquids.

6.4 Thixotropy

It explains how viscosity decreases over time when a constant shear stress is applied, and then slowly recovers as the material rests. This reversible behavior occurs due to the disruption and rebuilding of intermolecular networks within the bioink matrix, allowing for controlled flow during processing. Consequently, thixotropic materials show distinctive hysteresis loops in their flow curves, with the loop area representing the extent of structural breakdown. Moreover, unlike immediate shear-thinning responses, thixotropic behavior entails time-dependent structural changes that can be customized for particular bioprinting uses. Specifically, the recovery rate of thixotropic bioinks needs to be fine-tuned to ensure adequate flow during extrusion while also allowing quick structural restoration to preserve the printed shape. This time-dependent characteristic of rheological behavior is especially important for managing material properties during both the printing process and the following maturation stages [188–190] (Fig. 3).

7 Applications of 3D Bioprinting

Tissue engineering encompasses the interdisciplinary integration of clinical medicine, biomaterials, cell biology, molecular biology, bioengineering, and various other fields. This integration can be facilitated through the application of 3D bioprinting techniques, which enable the creation of replaceable tissues either *in vivo* or *in vitro*, aimed at restoring the functionality of damaged tissues and organs [191].

The application of biocompatible materials and cell-supporting components indicates significant potential for the restoration of the cancer microenvironment, tissue engineering, *in vitro* drug screening, wound healing, and the regeneration of skin and vascular tissues, among other uses. Moreover, 3D printing has accelerated the drug discovery process, aiding in the advancement through various phases and clinical trials [192]. Table 1 delivers a thorough summary of the numerous applications of 3D bioprinting within multiple areas of biomedicine.

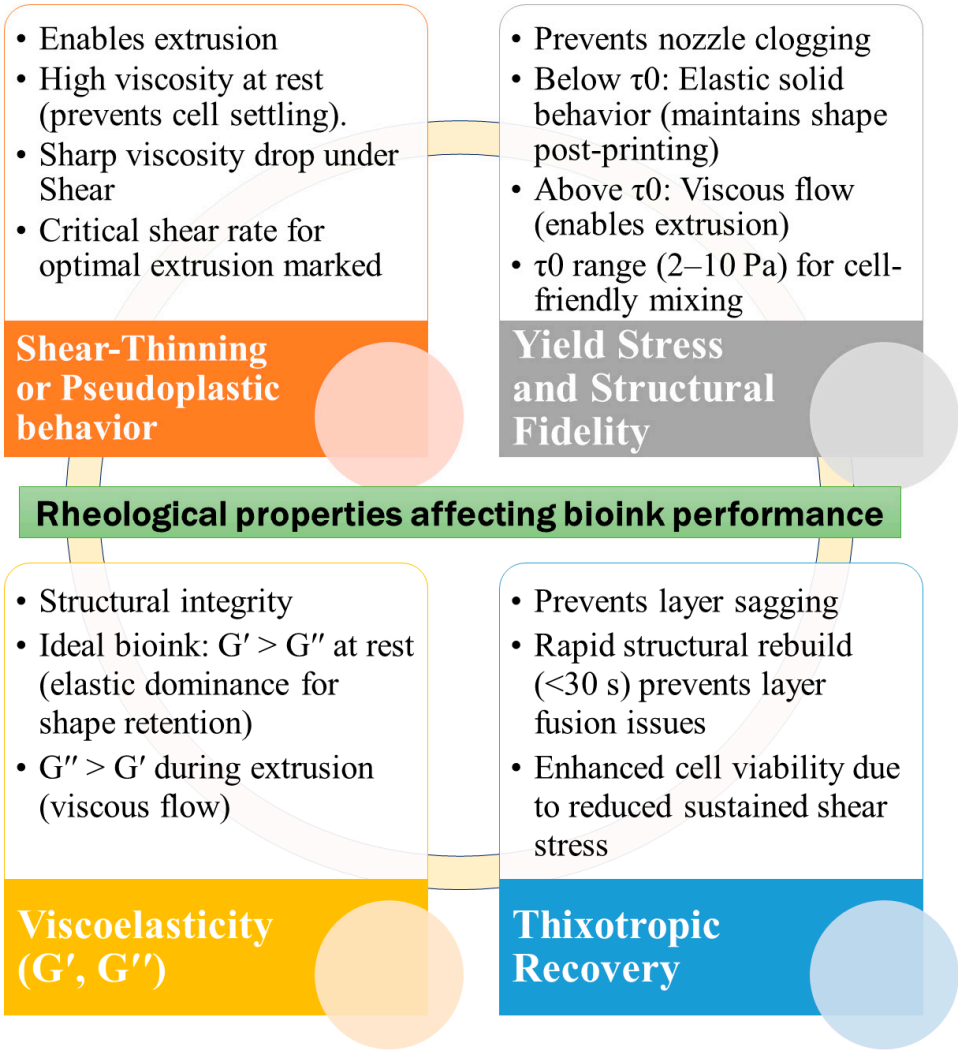

Figure 3: Fundamental Rheological Characteristics Influencing Bioink Functionality.

Table 1: Applications of 3D bioprinting.

Tissue Type	Type of Cells/Cellular Material	Bioink/Material Utilized	Bioprinting Strategy/Printer	Outcomes and Citations
Bone	Bone marrow mesenchymal stem cells (MSCs), osteoblast	Gelatin methacrylate (GelMA) hydrogel with nanocrystalline hydroxyapatite (nHA)	Stereolithography	An appropriate model for examining the interactive effects of cells within an artificial bone microenvironment is essential for investigating the progression of post-metastatic breast cancer in bone tissue [193].
	Osteoblast, breast cancer cells	HA nanoparticles into the PEG/PEG-DA resin	Table-top stereolithography	3D printed bone matrix can simulate tumour bone microenvironments and be used to research metastasis and drugs susceptibility [194].

Table 1: *Cont.*

Tissue Type	Type of Cells/Cellular Material	Bioink/Material Utilized	Bioprinting Strategy/Printer	Outcomes and Citations
Bone	Demineralized bone matrix (DBM)	Polycaprolactone (PCL), in combination with electrical stimulation (ES)	Stereolithography pneumatic printer (CELLINK)	The 3D-printed conductive scaffolds composed of DBM and enhanced through ES developed in this study more accurately replicate the characteristics of natural bone tissue. These scaffolds exhibit superior biological and electrical properties compared to existing synthetic bone scaffolds, thereby demonstrating their potential applicability in the field of bone tissue engineering [195].
	Decellularized bone matrix	Polycaprolactone	Stereolithography	Composite PCL/DCB scaffolds possess the requisite mechanical properties, structural geometry, and osteoinductive capabilities essential for use as TE bone grafts [196].
	human bone marrow-derived mesenchymal stem cell–derived matrisome (BMTS)	Collagen-fibrin/Polycaprolactone	Fused deposition modeling	BMTS-integrated 3D-printed scaffold improved tissue healing, osteoinduction, and bone formation in a rat calvarial model with a critical size deficit [197].
Skin	Decellularized extracellular matrices (dECMs)	dECM hydrogels	3D Discovery printer based on extrusion-based printing	Printed dECMs and cell tracking enable modeling of the early stages of metastatic illness, which may be utilized to better understand melanoma cell activity and drug response [198].
	Human foreskin fibroblasts (HFF-1), human umbilical vein endothelial cells (HUVECs), and human immortalized keratinocytes (HaCaTs)	Gelatin methacrylate (GelMA), oxidized hyaluronic acid (OHA), carboxymethyl chitosan (CMCS), and 2-methacryloyloxyethyl phosphorylcholine (MPC)	-	Conductive skin scaffolds offer a suitable conductive environment for cellular signaling, proliferation, migration, and differentiation, eventually accelerating the re-epithelialization, collagen deposition, and vascularization of skin wounds [199].
	Human amniotic epithelial cells (AECs) and Wharton's jelly derived mesenchymal stem cells (WJMSCs)	Alginate/gelatin composite hydrogels	Extrusion-based 3D bioprinting	High printing precision (151 ± 13.04 μm) and structural fidelity were achieved and expression of genes relating to re-epithelization and wound healing was significantly increased. Cell viability was more than 95% up to 6 days after printing [200].
	Keratinocyte and human dermal fibroblast cells	Crosslinked chitosan (CH)–genipin (GE)	Extrusion-based 3D bioprinting	The enhanced cell viability was achieved by the low printing pressure (20–40 kPA). The genipin-based crosslinking maintained 93% cell viability. Low print fidelity and cell spread [201].

Table 1: *Cont.*

Tissue Type	Type of Cells/Cellular Material	Bioink/Material Utilized	Bioprinting Strategy/Printer	Outcomes and Citations
Skin	HFBs and HUVECs (human umbilical cord)	PVA, nanocellulose, agarose, and sodium alginate	Extrusion-based 3D bioprinting	The tissue-engineered faces were designed with configurable sizes and shapes that can be vascularized. The use of PVA sacrificial layers might overcome the collapsing problem of hydrogel bioink in tissue size constructions. Vasculatoid traits led to the development of continuous vascular-like structures [202].
	Normal human dermal fibroblasts	PCL, silk sericin, Chitosan and Sodium alginate	Extrusion based bioprinting	Electrospun nanofibrous matrices were combined with 3D bioprinted constructions to imitate epidermis-dermis structures. The nanofiber layer provides antibacterial properties, while the printed layer creates a moist environment. Long-term monitoring is crucial for complete dermal-epidermal fusion [203].
Heart	Human-embryonic-stem-cell-derived cardiomyocytes (hESC-CMS) and CFs	Collagen	FRESH v2.0	Human heart components (ventricles, tri-leaflet heart valves, and vasculature) were fabricated. Neonatal-scale human heart with ventricles demonstrated synchronized contractions, directed action potential propagation, and wall thickening of up to 14% [204].
	Human induced pluripotent stem cell (hiPSC)-derived cardiomyocytes	Collagen-hyaluronic acid	Extrusion based bioprinting	The printed tissue demonstrated regular, spontaneous contractions that could withstand passive resistance and last for several months. Interestingly, pharmacological stimulation may be used to alter the printed cardiac tissues' heartbeat frequency [205].
	Neonatal mouse ventricular cardiomyocytes (NMVCMs)	Methacrylated gelatin (GelMA)	Microscale continuous optical printing (μCOP) system (Based on stereolithography)	Better alignment, synchronous beating, and physiological response were demonstrated by the printed microscale ventricular myocardium [167].
	iPSC-CMs (induced Pluripotent Stem Cell-derived Cardiomyocytes) and CFs (Cardiac Fibroblasts)	Heart tissue-derived extracellular matrix (hdECM)	Extrusion based bioprinting	The myocardial fiber orientations within a chamber-like structure, referred to as MoCha, demonstrated a mimicry of the native left ventricular architecture, characterized by synchronized contraction across its layers [206].
	Human induced pluripotent stem cell—derived cardiomyocytes (iPSC-CMs)	Poly (ethylene glycol) diacrylate	μCOP	Cardiac tissue exhibited improved maturation and indicated significant potential for high-throughput *in vitro* drug screening applications [207].

Table 1: *Cont.*

Tissue Type	Type of Cells/Cellular Material	Bioink/Material Utilized	Bioprinting Strategy/Printer	Outcomes and Citations
Heart	Human coronary artery endothelial cells (HCAECs)	Carbon nanotube-incorporated alginate framework	UV-integrated dispensing-based 3D-printing technique	The implanted cardiac patch demonstrated a high cell viability rate of 90% and exhibited superior electrical conductivity at physiologically relevant frequencies ranging from 1 to 5 Hz [208].
Liver	Decellularized liver matrix (dLM)	gelatin and polyethylene glycol	CellInk bioprinter	The 3D-printed construct demonstrated a high cell viability rate ranging from 85% to 93%, maintained liver-specific functions, and facilitated the proliferation of HepG2 cells, exhibiting liver-specific functionalities over a duration of 7 days [209].
	Human-induced pluripotent stem cells derived hepatocytes (hiPSC-Heps)	Alginate-gelatin	Extrusion based bioprinting	Higher mRNA expression of liver-specific activities, increased secretion of proteins linked to liver function, easier creation of hiPSC-Hep spheroids with increased viability and proliferation, and a positive therapeutic response were all demonstrated by the 3D-printed (3DP) model [210].
	Hepatic parenchymal cells, Huh7, HepaRG and hepatic stellate cells LX-2 cells	Methacrylated gelatin	Extrusion bioprinting process	Fibrillar collagen deposition was demonstrated in 3D multicellular bioprinted constructs made up of HepaRG, LX-2, and endothelial cells; which was not witnessed in monocultures of HepaRG or LX-2 alone. Complex interactions between the various hepatic cell types contributed to collagen deposition [211].
	Human adipose mesenchymal stem cell-derived hepatocyte-like cells (HLCs), human umbilical vein endothelial cells (HUVECs), and human hepatic stellate cells (HHSCs)	Liver extracellular matrix (ECM)	Extrusion-based bioprinting	The HLC/HUVEC/HHSC-loaded liver model exhibits increased cytochrome P450 (CPR) activity, urea synthesis, and albumin production, and it mimics natural alternating cords of hepatocytes with a functioning sinusoidal lumen-like network in both horizontal and vertical orientations [212].
	HepG2/C3A and EA.hy926 (immortalized human umbilical vein endothelial cell lines)	Collagen	Stereolithiography	Engineered multicellular structured spheroids demonstrated enhanced functionality and structural integrity. The *in vivo* Matrigel plug assay indicated that the structured spheroids exhibited greater stability and engraftment compared to their non-structured counterparts following transplantation [213].

Table 1: *Cont.*

Tissue Type	Type of Cells/Cellular Material	Bioink/Material Utilized	Bioprinting Strategy/Printer	Outcomes and Citations
Lung	Human lung fibroblasts (MRC-5), hybrid endothelial cells (EA.hy926) and airway epithelial cells (1HAEo-)	80% polyethylene glycol diacrylate (PEGDA) and 20% gelatin methacrylate (GelMa)	Stereolithographic (SLA) DLP bioprinting was performed using the LUMENX+ bioprinter (CELLINK; San Diego, California)	The apical epithelial and luminal endothelial layers were found to be intact in the 3D printed construct. Lung fibroblasts maintained 80–90% cell viability and their spindle structure with dendritic extensions. Distinct immune mediator profiles and clustering between co-cultures and tri-cultures at baseline were found by a multiplex test, highlighting variations in intercellular communication. A 3D bioprinted vascularized tri-culture model that replicates human airways was successfully constructed and characterized in this work [214].
	Human bronchial epithelial cells (BEAS-2B), human umbilical vein endothelial cells (HUVEC), human embryonic lung fibroblasts (MRC5), and human monocytes (THP-1)	Type I collagen functionalized Alg microspheres	3D-inkjet bioprinting	The artificial lung tissue structure with macrophages (ALTs@M) proved to be more effective than the standard artificial lung tissue structure (ALTs) in promoting the inflammatory microenvironment in the lungs. This offers a new *in vitro* model for studying cellular interactions and human macrophages. Overall, the construction strategy for this artificial lung tissue using 3D-inkjet bioprinting technology enables the adaptable creation of artificial lung tissue structures that could serve as potential disease models for preclinical research [215].
	Type I and II alveolar cells (NCI-H1703 and NCI-H441), lung fibroblasts (MRC5), and lung microvascular endothelial cells (HULEC-5a)	Collagen	Drop-on-demand inkjet printing	The 3D Alveolar Barrier Model provides a more accurate representation of the morphologies, structures, and functions of lung tissue. This thin multilayered model replicates actual tissue-level responses to influenza infection, and it is expected that this 3D alveolar barrier model can be utilized as an alternative to established test models for pathological and pharmaceutical objectives [216].
Neural	Neural stem cell (NSC)	SilMA (silk fibroin modified with glycidyl methacrylate)/Pectin/ MXene-soybean phospholipids (SP) bioink, where	Extrusion based bioprinting	Over 5 days, NSCs encapsulated in bioink showed maximal proliferation when electrically stimulated at 300 μA for 10 min every day. Neuronal differentiation was shown to be favorably linked with MXene-SP concentration and stimulation intensity. Electrical stimulation greatly increased synaptic activity and vesicle recycling. Electrical stimulation improved cell proliferation, neural differentiation, and synapse function [217].

Table 1: *Cont.*

Tissue Type	Type of Cells/Cellular Material	Bioink/Material Utilized	Bioprinting Strategy/Printer	Outcomes and Citations
Neural	Neural progenitor cells (NPCs) derived from human induced pluripotent stem cells (hiPSCs)	Gelatin Methacryloyl (GelMA)/Pluronic F127 (P-127)	Extrusion based bioprinting	The GelMA/P-127 composite bioinks shown excellent qualities for creating bioprinted structures capable of sustaining the prolonged proliferation of hiPSC-NPCs and promoting their differentiation into neurons and astrocytes. This capacity enables the creation of complex 3D brain tissue-like structures, creating a firm basis for testing potential therapies in CNS regenerative medicine [218].
	Neural stem cells (NSCs)	hydroxypropyl chitosan (HBC), thiolated hyaluronic acid (HA-SH), vinyl sulfonated hyaluronicacid (HA-VS) and matrigel (MA)	Microextrusion-based 3D printing system (Bioscaffolder, GeSim, Germany)	Fabricated scaffolds preserve high NSC survival (about 95%) and provide a benign environment that promotes cell-material interactions and proliferation of neurons, resulting in optimum neural network production. Additionally, the *in vivo* experiment revealed that the bioprinted scaffolds increased axon regeneration and reduced glial scar deposition, resulting in a notable locomotor recovery of the spinal cord injury model rats. This could be a general and malleable approach for precisely engineering the central nervous system and other neural organs/tissues for use in regenerative medicine [219].
Vascular grafts	Smooth muscle cells (SMCs) and fibroblasts (FCs)	Hyaluronic acid, gelatin, and polyethylene glycol diacrylate (PEGDA)	Organovo printer (extrusion-based 3D bioprinting)	The 3D-bioprinted vascular conduits that were implanted behaved physiologically like native vessels, were well-tolerated, and integrated effectively into the native vasculature. Advances in the treatment of vascular disease in humans are made possible by the fabrication and application of 3D-bioprinted vasculature for the repair of large vessels in an animal model [220].
	Human umbilical vein endothelial cells (HUVECs)	GelMA and gelatin	BIO X6 bioprinter (Cellink, USA)	The bioprinting procedure did not significantly impact cell survival, according to cell viability tests. The functioning of the printed channels was successfully demonstrated, and by adding HUVECs to the core region, it was possible to create micro-vessels inside the printed scaffolds. Following incubation, HUVECs coated the inner walls of the GelMA shells, creating microvessels with lumens [221].

Table 1: *Cont.*

Tissue Type	Type of Cells/Cellular Material	Bioink/Material Utilized	Bioprinting Strategy/Printer	Outcomes and Citations
Vascular grafts	Decellularized extracellular matrix (dECM)	Nano clay (NC)/sodium alginate (SA)	Coaxial 3D bioprinting	Tubular scaffold having unique structures and functions that direct fibroblast and endothelial cell adhesion and proliferation while also facilitating tissue repair and reconstruction. The combination of calcium alginate and nano clay enhanced the mechanical strength and stability of the tubular scaffolds, which was vital for blood vessel regeneration [222].
Cartilage	Adipose-derived mesenchymal stem/stromal cells (ADSCs)	-	Bio-3D printer	Cartilage constructions with mechanical and histological attributes similar to articular cartilage were successfully produced. In addition, thick cartilage constructions developed with completely grown deep layers. ADSCs with 3D printing technology may be used to generate patient-specific constructions, which can assist in developing human-sized cartilage constructs [223].
	Human chondrocytes (hACs)	Gelatin methacrylate (GelMA)/GelMA functionalized with a fluorinated oxadiazole (GelOXA)	CellInk bioprinter	The GelMA/GelOXA scaffold retained hAC viability, maintained their natural phenotype, and substantially enhanced type II collagen synthesis, paving the path for the regeneration of healthy, hyaline-like cartilage by supplying hypoxia signals even under normoxic settings. Moreover, Osteoarthritis and associated chondral defects may be effectively treated by the GelMA/GelOXA scaffold's capacity to send healing signals straight to the site of injury [224].
	Bone marrow mesenchymal stem cells (BMSCs)	Decalcified bone matrix (DBM)-Gelatin	-	DBM-GT demonstrated enhanced pore structure and mechanical characteristics, including both dry and wet mechanical strength. Chondrocytes suppressed osteogenic differentiation while encouraging chondrogenic differentiation, leading to the successful regeneration of stable cartilage both *in vitro* and *in vivo*, as well as the formation of complex chondrofibrous tissues resembling tracheal structures [225].
	Mesenchymal stem cells (MSCs)	PCL/GelMa	Cellink gothenburg Sweden	*In vitro* cartilage regeneration was feasible with a 3D bioprinted scaffold. In a ferret model of laryngotracheal reconstruction (LTR), *in vivo* implantation of these 3D bioprinted scaffolds revealed effective healing of the defect area, formation of epithelial mucosa in the inner lumen, and an increase in airway volume [226].

8 Current Challenges in Biomaterials' Clinical Translation and Potential Solutions

The majority of bioprinted tissues and organs are relatively small, comprising only one or two types of cells, featuring fairly simple structures, and offering limited functionality. Typically, bioprinted tissues do not possess vascular networks, thereby depending on diffusion for the delivery of nutrients. To achieve the bioprinting of larger and more complex tissues with durable, customizable mechanical properties and materials that are compatible with cells, it is essential to develop methods for deriving and expanding various types of functional, progenitor, and supporting cell types, in addition to strategies for integrating a vascular network to facilitate oxygen and nutrient supply. Table 2 tabulates the current challenges in biomaterial's utilization.

Table 2: Current obstacles in the 3D bioprinting and prospective remedies.

	Current Obstacles	Prospective Remedies
Bioinks	Precise replication of the functional and biomechanical characteristics of tissue	Hybrid constructs featuring patterned synthetic and natural materials (including ECM-derived hydrogels): the synthetic materials contribute to physical integrity and facilitate control over the scaffold's mechanical, structural, and geometrical properties (such as elastic modulus, tensile strength, porosity, and alignment) at the macroscopic scale, while the natural materials provide a conducive structural and biochemical environment for cell encapsulation and placement [227,228]
	Compatible attributes for bioprinter deposition	ECM-based hydrogels [229–231]
	Reliable and adjustable mechanical properties after printing	Modification of ECM and hydrogel materials, either chemically or non-chemically [232–235]
	Physiological, biochemical, and mechanical interactions with cellular elements	Synthetic peptides that imitate ECM func-tional motifs [236–238]
	Appropriate degradation times for scaffolds	'Smart' materials whose characteristics evolve over time or following external stimuli [239–242]
Cell sourcing	Cell sourcing techniques that are minimally invasive or entirely non-invasive	Utilization of small molecules to regulate cell function, exemplified by conditional cell reprogramming [243–245]
	Cell sources that are either autologous or lack immunogenicity	Mesenchymal cells [246,247] Induced pluripotent stem cells [248–251] Perinatal/adipose-derived cells [252–254]
Vascularization	The distribution of oxygen and nutrients in dense tissues	Embedding in microchannel [255–257]
	Fabrication of multiscale hierarchical networks characterized by complex structures	Patterning of angiogenic growth factors or cells [258,259]
	Direct fabrication of vascular elements or the patterning of cells and/or factors that mature either *in vivo* or in bioreactors	Sacrificial templates for the construction of perfusable microchannel networks [260,261] Direct bioprinting of vascular networks through cell patterning or tissue spheroids [262,263]

9 Flow Regimes, Rheological Challenges, and Transport Phenomena in Bio-Ink Deposition

Bio-ink deposition forms the core of 3D bioprinting, where cell-laden hydrogels or matrices are precisely extruded layer-by-layer to build functional tissue constructs. This process relies on controlled flow through nozzles, crosslinking for shape fidelity, and biocompatibility to preserve cell viability above 80–90% post-printing. Pre-bioprinting involves designing digital models from medical scans and preparing bio-ink by mixing cells, biomaterials like alginate or gelatin, and nutrients. During bioprinting, the cartridge extrudes bio-ink via pneumatic pressure or mechanical screws onto a moving stage, following x-y-z coordinates to form scaffolds. Post-bioprinting includes maturation in incubators, where constructs solidify via UV light, ionic crosslinking (e.g., Ca^{2+} for alginate), or temperature shifts, enabling self-assembly into tissues. Bio-inks must exhibit shear-thinning rheology for smooth flow, yield stress to prevent settling, and rapid gelation for filament stability. Common formulations include GelMA (gelatin methacryloyl) at 10% with 1.5×10^6 cells/mL, crosslinked by UV, balancing printability and mechanical strength. Challenges like cell viability drop with higher viscosity (e.g., 6% alginate) highlight trade-offs in extrusion pressure and nozzle design [264].

9.1 Flow Regimes

Bio-inks typically exhibit laminar flow in extrusion nozzles due to low Reynolds numbers from high viscosities, with velocity peaking at the centerline and dropping to zero at walls (Fig. 4). In cylindrical nozzles, flow accelerates sharply in tapered sections, reaching steady-state where pressure gradients balance viscous forces; conical nozzles show exponential velocity increases, amplifying centerline speeds by up to 1.5 times. Disruptions like secondary flows from cell sedimentation can induce turbulence, degrading filament uniformity, though most processes maintain Reynolds <2000 for stability [265,266]. Bioinks follow parabolic velocity profiles in cylindrical nozzles, with maximum speed at the centerline and zero at walls, accelerating in tapered sections to balance pressure gradients and viscous forces. Conical nozzles yield higher outlet velocities (up to 1.5× faster) and steadier flow at lower pressures, minimizing shear stress buildup that peaks near walls (10–100 kPa). Shear-thinning rheology dominates, transitioning shear stress to tensile under high flow rates. Laminar regimes preserve cell viability by limiting turbulence-induced damage, while jetting ensures uniform deposition for scaffolds. Disruptions from cell sedimentation or air entrainment can induce secondary flows, addressed via yield stress >10 Pa and thixotropy [267]. Laminar regimes preserve cell viability by limiting turbulence-induced damage, while jetting ensures uniform deposition for scaffolds. Disruptions from cell sedimentation or air entrainment can induce secondary flows, addressed via yield stress >10 Pa and thixotropy.

9.2 Rheological Challenges

Ideal bio-inks display shear-thinning (viscosity decreases with shear rate), yield stress (minimum stress for flow, ~10–1000 Pa), and thixotropy (time-dependent viscosity recovery post-shear) (Fig. 4). These properties prevent cell settling at rest (high zero-shear viscosity $>10^3$ Pa·s) while enabling extrusion at moderate pressures ($G' > G''$ for elastic dominance). Challenges arise from trade-offs: high yield stress aids shape fidelity but resists flow; temperature-sensitive gels like gelatin must gelate rapidly post-deposition without nozzle clogging, often mitigated by additives like Carbopol [188,268]. Ideal bioinks exhibit non-Newtonian traits: power-law index $n < 1$ for shear-thinning, storage modulus G' > loss modulus G'' at low strains for elasticity, and thixotropy for viscosity recovery post-shear. Viscoelasticity ensures filament stability without spreading, as seen in alginate-CMC blends where higher CMC reduces filament width via enhanced shear-thinning. Trade-offs include rapid gelation (e.g., via Ca^{2+} crosslinking) conflicting with biocompatibility, limiting nutrient diffusion in stiff gels. High shear stress at nozzle walls (up to

3.7 kPa) creates spatial viability gradients, with HEK 293 cells showing 90% survival but edge damage in filaments. Additives like laponite induce cell aggregation in viscous inks, disrupting uniform distribution and proliferation. Optimizing via rotational rheology and creep tests correlates flow profiles to printability, targeting zero-shear viscosity >10^3 Pa·s for stability [189,269].

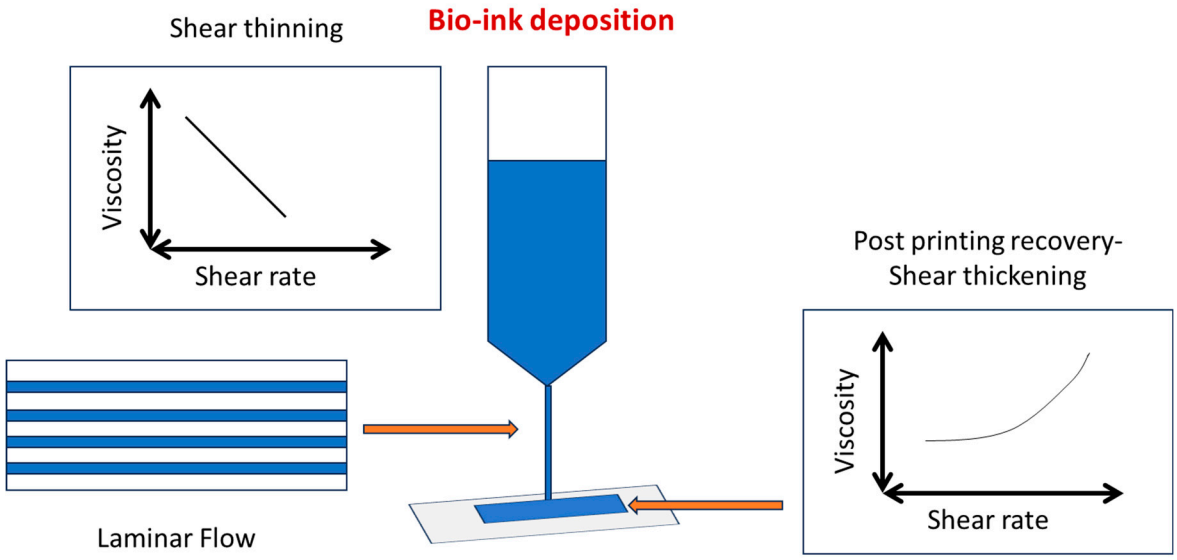

Figure 4: Flow regime and Rheological behaviour in bio-ink deposition.

9.3 Transport Phenomena

Transport phenomena in bioink deposition during 3D bioprinting govern mass, momentum, and heat transfer, influencing cell survival, nutrient diffusion, and structural integrity from nozzle extrusion to scaffold formation. Convection dominates inside nozzles via bulk flow, while diffusion prevails post-deposition in hydrogels, limited to ~100–200 μm depths due to low diffusivity in viscous matrices. During deposition, convective transport dominates via bulk flow, transitioning to diffusion post-extrusion for oxygen/nutrient penetration limited to ~100–200 μm in hydrogels. Shear stresses (up to 10–100 kPa near walls) risk cell damage, with tensile stresses peaking axially in nozzles under high flow rates. Mass transfer models like Herschel-Bulkley describe non-Newtonian behavior, where Peclet numbers >1 favor convection over diffusion, influencing bio-ink crosslinking and scaffold porosity [265,270,271].

Shear stresses peak near nozzle walls (10–100 kPa), driven by parabolic velocity profiles and non-Newtonian rheology, risking cell membrane rupture above 0.5–1 kPa thresholds. Laminar flow (Re < 2000) at low velocities minimizes turbulence, but secondary flows from cell sedimentation disrupt uniformity, modeled via Navier-Stokes equations for Herschel-Bulkley fluids. Pre-extrusion convection delivers nutrients uniformly, transitioning to Fickian diffusion post-deposition where Peclet numbers >1 favor advection initially. Crosslinking (e.g., UV or ionic) creates gradients, with oxygen penetration hindered in dense gels, necessitating porous designs or sacrificial inks for vascular-like channels. Thermal gradients in thermoplastic bioinks induce localized gelation, while photoinitiators in DLP limit curing depth via light absorption, preventing overcuring. High cell densities slow gelation kinetics, altering viscoelastic moduli and impacting long-term mass transport in maturing constructs [185,271].

10 Perspectives and Conclusion

The advancement of 3D printing and biology has unveiled modern bearings in tissue regeneration and organ development amid the last decade. Indeed, in spite of the fact that this strategy could be a generally early organize of advancement, 3D bioprinting tissue with this strategy has appeared incredible promise. Additional progress for 3D Printing technologies is required to enhance the structure resolution, preserving the cell viability, and diminishing the manufacturing time without relinquishing the shape, quality, and usability of platforms. This review gives an outline of the foremost common and novel biomaterials in 3D bioprinting technology, assisting in presenting the related strategies that are commonly taken into consideration by researchers. In expansion, an endeavor has been fulfilled to hand over the foremost significant application of 3D bioprinting strategies, which incorporate the fabrication of bone, cartilage, vascular grafts, skin, neural, heart, liver, and lung tissue. In order to conduct a comparison using existing biomaterials and 3D bioprinting processes, we paid particular attention to highlighting their pros and cons. Due to the fast-paced advancements in 3D bioprinting technology, additional investigation is needed to maintain its viability as a manufacturing tool in biomedical systems.

Acknowledgement: Not applicable.

Funding Statement: The authors received no specific funding for this study.

Author Contributions: The authors confirm contribution to the paper as follows: Priyadarshini Patel: Writing, Formatting, Komal Parmar: Writing, Editing. All authors reviewed the results and approved the final version of the manuscript.

Availability of Data and Materials: The data that support the findings of this study are available from the Corresponding Author, [Komal Parmar], upon reasonable request.

Ethics Approval: Not applicable.

Conflicts of Interest: The authors declare no conflicts of interest to report regarding the present study.

References

1. Woodward D. Review of the printing press as an agent of change, by Elizabeth L. Eisenstein. Imago Mundi. 1980;32:95–7. [CrossRef].
2. Wang K, Lin H, Fang N, Xu J, Zhang S, Tan J, et al. Cross-patch graph transformer enforced by contrastive information fusion for energy demand forecasting towards sustainable additive manufacturing. J Ind Inf Integr. 2025;45:100795. [CrossRef].
3. Gibson I, Rosen D, Stucker B, Khorasani M. Development of additive manufacturing technology. In: Additive Manufacturing Technologies. Cham, Switzerland: Springer International Publishing; 2020. p. 23–51. [CrossRef].
4. Bhatti SS, Singh J. 3D printing of biomaterials for biomedical applications: a review. Int J Interact Des Manuf. 2023. [CrossRef].
5. Atala A. Introduction: 3D printing for biomaterials. Chem Rev. 2020;120:10545–6. [CrossRef].
6. Berman B. 3-D printing: the new industrial revolution. Bus Horiz. 2012;55(2):155–62. [CrossRef].
7. Rossi S, Puglisi A, Benaglia M. Additive manufacturing technologies: 3D printing in organic synthesis. ChemCatChem. 2018;10(7):1512–25. [CrossRef].
8. Jose RR, Rodriguez MJ, Dixon TA, Omenetto F, Kaplan DL. Evolution of bioinks and additive manufacturing technologies for 3D bioprinting. ACS Biomater Sci Eng. 2016;2(10):1662–78. [CrossRef].
9. Jose RR, Brown JE, Polido KE, Omenetto FG, Kaplan DL. Polyol-silk bioink formulations as two-part room-temperature curable materials for 3D printing. ACS Biomater Sci Eng. 2015;1(9):780–8. [CrossRef].
10. Oliveira SM, Reis RL, Mano JF. Towards the design of 3D multiscale instructive tissue engineering constructs: current approaches and trends. Biotechnol Adv. 2015;33(6):842–55. [CrossRef].

11. Zadpoor A. Design for additive bio-manufacturing: from patient-specific medical devices to rationally designed meta-biomaterials. Int J Mol Sci. 2017;18(8):1607. [CrossRef].
12. Ford S, Despeisse M. Additive manufacturing and sustainability: an exploratory study of the advantages and challenges. J Clean Prod. 2016;137:1573–87. [CrossRef].
13. Goyanes A, Fina F, Martorana A, Sedough D, Gaisford S, Basit AW. Development of modified release 3D printed tablets (printlets) with pharmaceutical excipients using additive manufacturing. Int J Pharm. 2017;527(1–2):21–30. [CrossRef].
14. Bartlett S. Printing organs on demand. Lancet Respir Med. 2013;1(9):684. [CrossRef].
15. Ben-Ner A, Siemsen E. Decentralization and localization of production. Calif Manage Rev. 2017;59(2):1–19. [CrossRef].
16. Lee SJ, Jeong W, Atala A. 3D bioprinting for engineered tissue constructs and patient-specific models: current progress and prospects in clinical applications. Adv Mater. 2024;36(49):2408032. [CrossRef].
17. Poluri N, Carter J, Grasso J, Miller W, Leinbach M, Durant F, et al. New frontiers in 3D printing using biocompatible polymers. Int J Mol Sci. 2025;26(16):8016. [CrossRef].
18. Sultana N. Mechanical and biological properties of scaffold materials. In: Deng Y, Kuiper J, editors. Functional 3D tissue engineering scaffolds. Amsterdam, The Netherlands: Elsevier; 2018. p. 1–21. [CrossRef].
19. Włodarczyk-Biegun MK, del Campo A. 3D bioprinting of structural proteins. Biomaterials. 2017;134:180–201. [CrossRef].
20. Steenhuis HJ, Pretorius L. The additive manufacturing innovation: a range of implications. J Manuf Technol Manag. 2017;28(1):122–43. [CrossRef].
21. Chen Q, Liang S, Thouas GA. Elastomeric biomaterials for tissue engineering. Prog Polym Sci. 2013;38(3–4):584–671. [CrossRef].
22. van Vugt TA, Geurts JAP, Arts JJ, Lindfors NC. Biomaterials in treatment of orthopedic infections. In: Management of periprosthetic joint infections (PJIs). Amsterdam, The Netherlands: Elsevier; 2017. p. 41–68. [CrossRef].
23. Ma PX. Scaffolds for tissue fabrication. Mater Today. 2004;7(5):30–40. [CrossRef].
24. Sultana N, Hassan MI, Lim MM, Sultana N, Hassan MI, Lim MM. Scaffolding biomaterials. In: Composite Synthetic Scaffolds for Tissue Engineering and Regenerative Medicine. Cham, Switzerland: Springer International Publishing; 2015. p. 1–11. [CrossRef].
25. Asadi N, Del Bakhshayesh AR, Davaran S, Akbarzadeh A. Common biocompatible polymeric materials for tissue engineering and regenerative medicine. Mater Chem Phys. 2020;242:122528. [CrossRef].
26. Udenni Gunathilake T, Ching Y, Ching K, Chuah C, Abdullah L. Biomedical and microbiological applications of bio-based porous materials: a review. Polymers. 2017;9(5):160. [CrossRef].
27. Tejera M, Galiç S, Lavicza Z. 3D modelling and printing in teacher education: a systematic literature review. J STEM Educ Res. 2025. [CrossRef].
28. Kodama H. Automatic method for fabricating a three-dimensional plastic model with photo-hardening polymer. Rev Sci Instrum. 1981;52(11):1770–3. [CrossRef].
29. Hull CW, inventor; 3D Systems Inc., assignee. Apparatus for production of three-dimensional objects by stereolithography. United States patent US 638,905. 1984 Aug 8.
30. Wang X, Jiang M, Zhou Z, Gou J, Hui D. 3D printing of polymer matrix composites: a review and prospective. Compos Part B Eng. 2017;110:442–58. [CrossRef].
31. Bartolo PJ, Gaspar J. Metal filled resin for stereolithography metal part. CIRP Ann. 2008;57(1):235–8. [CrossRef].
32. Halloran JW. Ceramic stereolithography: additive manufacturing for ceramics by photopolymerization. Annu Rev Mater Res. 2016;46:19–40. [CrossRef].
33. Deshmane S, Kendre P, Mahajan H, Jain S. Stereolithography 3D printing technology in pharmaceuticals: a review. Drug Dev Ind Pharm. 2021;47(9):1362–72. [CrossRef].
34. Mironov V, Kasyanov V, Markwald RR. Organ printing: from bioprinter to organ biofabrication line. Curr Opin Biotechnol. 2011;22(5):667–73. [CrossRef].
35. Bandyopadhyay A, Ghosh S, Boccaccini AR, Bose S. 3D printing of biomedical materials and devices. J Mater Res. 2021;36(19):3713–24. [CrossRef].
36. Chocholata P, Kulda V, Babuska V. Fabrication of scaffolds for bone-tissue regeneration. Materials. 2019;12(4):568. [CrossRef].

37. Mathew AP, Augustine R, Kalarikkal N, Thomas S. Tissue engineering: Principles, recent trends and the future. In: Nanomedicine and tissue engineering: state of the art and recent trends. Waretown, NJ, USA: Apple Academic Press; 2016. [CrossRef].
38. Perić Kačarević Ž, Rider P, Alkildani S, Retnasingh S, Pejakić M, Schnettler R, et al. An introduction to bone tissue engineering. Int J Artif Organs. 2020;43(2):69–86. [CrossRef].
39. Roseti L, Parisi V, Petretta M, Cavallo C, Desando G, Bartolotti I, et al. Scaffolds for Bone Tissue Engineering: state of the art and new perspectives. Mater Sci Eng C. 2017;78:1246–62. [CrossRef].
40. Verma P, Verma V. Concepts of Tissue Engineering. In: Verma AS, Singh A, editors. Animal Biotechnology. San Diego, CA, USA: Academic Press; 2014. p. 233–45. [CrossRef].
41. Williams DF. On the mechanisms of biocompatibility. Biomaterials. 2008;29(20):2941–53. [CrossRef].
42. Eldeeb AE, Salah S, Elkasabgy NA. Biomaterials for tissue engineering applications and current updates in the field: a comprehensive review. AAPS PharmSciTech. 2022;23(7):267. [CrossRef].
43. Nikolova MP, Chavali MS. Recent advances in biomaterials for 3D scaffolds: a review. Bioact Mater. 2019;4:271–92. [CrossRef].
44. Dee KC, Puleo DA, Bizios R. An introduction to tissue-biomaterial interactions. Cell Mol Biol. 2004;8:419–25. [CrossRef].
45. Roberts TT, Rosenbaum AJ. Bone grafts, bone substitutes and orthobiologics: the bridge between basic science and clinical advancements in fracture healing. Organogenesis. 2012;8(4):114–24. [CrossRef].
46. O'Brien FJ. Biomaterials & scaffolds for tissue engineering. Mater Today. 2011;14(3):88–95. [CrossRef].
47. Sabree I, Gough JE, Derby B. Mechanical properties of porous ceramic scaffolds: influence of internal dimensions. Ceram Int. 2015;41(7):8425–32. [CrossRef].
48. Gurumurthy B, Janorkar AV. Improvements in mechanical properties of collagen-based scaffolds for tissue engineering. Curr Opin Biomed Eng. 2021;17:100253. [CrossRef].
49. Chan BP, Leong KW. Scaffolding in tissue engineering: general approaches and tissue-specific considerations. Eur Spine J. 2008;17(4):467–79. [CrossRef].
50. Francois EL, Yaszemski MJ. Preclinical bone repair models in regenerative medicine. In: Principles of regenerative medicine. Amsterdam, The Netherlands: Elsevier; 2019. p. 761–7. [CrossRef].
51. Rahmani Del Bakhshayesh A, Mostafavi E, Alizadeh E, Asadi N, Akbarzadeh A, Davaran S. Fabrication of three-dimensional scaffolds based on nano-biomimetic collagen hybrid constructs for skin tissue engineering. ACS Omega. 2018;3(8):8605–11. [CrossRef].
52. Yetiskin B, Okay O. High-strength silk fibroin scaffolds with anisotropic mechanical properties. Polymer. 2017;112:61–70. [CrossRef].
53. Osidak EO, Kozhukhov VI, Osidak MS, Domogatsky SP. Collagen as bioink for bioprinting: a comprehensive review. Int J Bioprinting. 2020;6(3):270. [CrossRef].
54. Kiyotake EA, Douglas AW, Thomas EE, Nimmo SL, Detamore MS. Development and quantitative characterization of the precursor rheology of hyaluronic acid hydrogels for bioprinting. Acta Biomater. 2019;95:176–87. [CrossRef].
55. Hauptstein J, Forster L, Nadernezhad A, Groll J, Teßmar J, Blunk T. Tethered TGF-β1 in a hyaluronic acid-based bioink for bioprinting cartilaginous tissues. Int J Mol Sci. 2022;23(2):924. [CrossRef].
56. Law N, Doney B, Glover H, Qin Y, Aman ZM, Sercombe TB, et al. Characterisation of hyaluronic acid methylcellulose hydrogels for 3D bioprinting. J Mech Behav Biomed Mater. 2018;77:389–99. [CrossRef].
57. Xu C, Hung C, Cao Y, Liu HH. Tunable crosslinking, reversible phase transition, and 3D printing of hyaluronic acid hydrogels via dynamic coordination of innate carboxyl groups and metallic ions. ACS Appl Bio Mater. 2021;4(3):2408–28. [CrossRef].
58. Noh I, Kim N, Tran HN, Lee J, Lee C. 3D printable hyaluronic acid-based hydrogel for its potential application as a bioink in tissue engineering. Biomater Res. 2019;23:3. [CrossRef].
59. Hakam MS, Imani R, Abolfathi N, Fakhrzadeh H, Sharifi AM. Evaluation of fibrin-gelatin hydrogel as biopaper for application in skin bioprinting: an *in-vitro* study. Bio Med Mater Eng. 2017;27(6):669–82. [CrossRef].
60. England S, Rajaram A, Schreyer DJ, Chen X. Bioprinted fibrin-factor XIII-hyaluronate hydrogel scaffolds with encapsulated Schwann cells and their *in vitro* characterization for use in nerve regeneration. Bioprinting. 2017;5:1–9. [CrossRef].
61. Sahranavard M, Zamanian A, Ghorbani F, Shahrezaee MH. A critical review on three dimensional-printed chitosan hydrogels for development of tissue engineering. Bioprinting. 2020;17:e00063. [CrossRef].

62. Tarassoli SP, Jessop ZM, Kyle S, Whitaker IS. Candidate bioinks for 3D bioprinting soft tissue. In: 3D bioprinting for reconstructive surgery. Amsterdam, The Netherlands: Elsevier; 2018. p. 145–72. [CrossRef].
63. Taghizadeh M, Taghizadeh A, Yazdi MK, Zarrintaj P, Stadler FJ, Ramsey JD, et al. Chitosan-based inks for 3D printing and bioprinting. Green Chem. 2022;24(1):62–101. [CrossRef].
64. Wang X, Ao Q, Tian X, Fan J, Tong H, Hou W, et al. Gelatin-based hydrogels for organ 3D bioprinting. Polymers. 2017;9(9):401. [CrossRef].
65. Asim S, Tabish TA, Liaqat U, Ozbolat IT, Rizwan M. Advances in gelatin bioinks to optimize bioprinted cell functions. Adv Healthc Mater. 2023;12(17):2203148. [CrossRef].
66. Sultan MT, Lee OJ, Lee JS, Park CH. Three-dimensional digital light-processing bioprinting using silk fibroin-based bio-ink: recent advancements in biomedical applications. Biomedicines. 2022;10(12):3224. [CrossRef].
67. Park TY, Yang YJ, Ha DH, Cho DW, Cha HJ. Marine-derived natural polymer-based bioprinting ink for biocompatible, durable, and controllable 3D constructs. Biofabrication. 2019;11(3):035001. [CrossRef].
68. Axpe E, Oyen M. Applications of alginate-based bioinks in 3D bioprinting. Int J Mol Sci. 2016;17(12):1976. [CrossRef].
69. Rastogi P, Kandasubramanian B. Review of alginate-based hydrogel bioprinting for application in tissue engineering. Biofabrication. 2019;11(4):042001. [CrossRef].
70. Piras CC, Smith DK. Multicomponent polysaccharide alginate-based bioinks. J Mater Chem B. 2020;8(36):8171–88. [CrossRef].
71. Liu F, Wang X. Synthetic polymers for organ 3D printing. Polymers. 2020;12(8):1765. [CrossRef].
72. Khoeini R, Nosrati H, Akbarzadeh A, Eftekhari A, Kavetskyy T, Khalilov R, et al. Natural and synthetic bioinks for 3D bioprinting. Adv NanoBiomed Res. 2021;1(8):2000097. [CrossRef].
73. Lee TT, García JR, Paez JI, Singh A, Phelps EA, Weis S, et al. Light-triggered *in vivo* activation of adhesive peptides regulates cell adhesion, inflammation and vascularization of biomaterials. Nature Mater. 2015;14(3):352–60. [CrossRef].
74. Irukuvarjula V, Fouladgar F, Powell R, Carney E, Habibi N. Bioprinting 3D lattice-structured lumens using polyethylene glycol diacrylate (PEGDA) combined with self-assembling peptide nanofibers as hybrid bioinks for anchorage dependent cells. OpenNano. 2025;21:100223. [CrossRef].
75. Xin S, Chimene D, Garza JE, Gaharwar AK, Alge DL. Clickable PEG hydrogel microspheres as building blocks for 3D bioprinting. Biomater Sci. 2019;7(3):1179–87. [CrossRef].
76. Peak CW, Singh KA, Adlouni M, Chen J, Gaharwar AK. Printing therapeutic proteins in 3D using nanoengineered bioink to control and direct cell migration. Adv Healthc Mater. 2019;8(11):1801553. [CrossRef].
77. Upadhyay P, Gupta MK, Upadhyay S. Bioink Technology in 3D Bioprinting and Their Improvement In Handbook of 3D printing in biomedical applications. Boca Raton, FL, USA: CRC Press; 2025. [CrossRef].
78. Um JH, Park JH, Kim TH, Park SH, Mun J, Kang EH, et al. 3D-printed scaffolds for ear reconstruction using decellularized human cartilage-derived bioink and polycaprolactone. ACS Biomater Sci Eng. 2025;11(5):2834–45. [CrossRef].
79. Numpaisal PO, Jeencham R, Ponchana S, Ruksakulpiwat Y. Zone specific 3D-printed *Meniscus* scaffold from nanohydroxyapatite-reinforced polycaprolactone/hydrogel bioinks. Eur Polym J. 2025;230:113899. [CrossRef].
80. Mousavi Nejad Z, Zamanian A, Saeidifar M, Vanaei HR, Salar Amoli M. 3D bioprinting of polycaprolactone-based scaffolds for pulp-dentin regeneration: investigation of physicochemical and biological behavior. Polymers. 2021;13(24):4442. [CrossRef].
81. Tsai YC, Li S, Hu SG, Chang WC, Jeng US, Hsu SH. Synthesis of thermoresponsive amphiphilic polyurethane gel as a new cell printing material near body temperature. ACS Appl Mater Interfaces. 2015;7(50):27613–23. [CrossRef].
82. Hsieh FY, Hsu SH. 3D bioprinting: a new insight into the therapeutic strategy of neural tissue regeneration. Organogenesis. 2015;11(4):153–8. [CrossRef].
83. Hsieh FY, Lin HH, Hsu SH. 3D bioprinting of neural stem cell-laden thermoresponsive biodegradable polyurethane hydrogel and potential in central nervous system repair. Biomaterials. 2015;71:48–57. [CrossRef].
84. Ho L, Hsu SH. Cell reprogramming by 3D bioprinting of human fibroblasts in polyurethane hydrogel for fabrication of neural-like constructs. Acta Biomater. 2018;70:57–70. [CrossRef].

85. Olmos-Juste R, Larrañaga-Jaurrieta G, Larraza I, Ramos-Diez S, Camarero-Espinosa S, Gabilondo N, et al. Alginate-waterborne polyurethane 3D bioprinted scaffolds for articular cartilage tissue engineering. Int J Biol Macromol. 2023;253:127070. [CrossRef].
86. Kurakula M, Koteswara Rao GSN. Moving polyvinyl pyrrolidone electrospun nanofibers and bioprinted scaffolds toward multidisciplinary biomedical applications. Eur Polym J. 2020;136:109919. [CrossRef].
87. Ng WL, Huang X, Shkolnikov V, Suntornnond R, Yeong WY. Polyvinylpyrrolidone-based bioink: influence of bioink properties on printing performance and cell proliferation during inkjet-based bioprinting. Bio Des Manuf. 2023;6(6):676–90. [CrossRef].
88. Izgordu MS, Uzgur EI, Ulag S, Sahin A, Karademir Yilmaz B, Kilic B, et al. Investigation of 3D-printed polycaprolactone-/polyvinylpyrrolidone-based constructs. Cartilage. 2021;13(2_suppl):626S–35S. [CrossRef].
89. Ng W, Yeong W, Naing M. Polyvinylpyrrolidone-based bio-ink improves cell viability and homogeneity during drop-on-demand printing. Materials. 2017;10(2):190. [CrossRef].
90. Rasal RM, Janorkar AV, Hirt DE. Poly(lactic acid) modifications. Prog Polym Sci. 2010;35(3):338–56. [CrossRef].
91. González-Rodríguez L, Pérez-Davila S, Lama R, López-Álvarez M, Serra J, Novoa B, et al. 3D printing of PLA:CaP:GO scaffolds for bone tissue applications. RSC Adv. 2023;13(23):15947–59. [CrossRef].
92. Pant S, Thomas S, Loganathan S, Valapa RB. 3D bioprinted poly(lactic acid)/mesoporous bioactive glass based biomimetic scaffold with rapid apatite crystallization and *in-vitro* Cytocompatability for bone tissue engineering. Int J Biol Macromol. 2022;217:979–97. [CrossRef].
93. Kolan KCR, Semon JA, Bindbeutel AT, Day DE, Leu MC. Bioprinting with bioactive glass loaded polylactic acid composite and human adipose stem cells. Bioprinting. 2020;18:e00075. [CrossRef].
94. Sun F, Sun X, Wang H, Li C, Zhao Y, Tian J, et al. Application of 3D-printed, PLGA-based scaffolds in bone tissue engineering. Int J Mol Sci. 2022;23(10):5831. [CrossRef].
95. Guo T, Lim CG, Noshin M, Ringel JP, Fisher JP. 3D printing bioactive PLGA scaffolds using DMSO as a removable solvent. Bioprinting. 2018;10:e00038. [CrossRef].
96. Teo YC, Abbas A, Park EJ, Barbut C, Guo J, Goh D, et al. 3D printed bioactive PLGA dermal scaffold for burn wound treatment. ACS Mater Au. 2023;3(3):265–72. [CrossRef].
97. Song X, Li X, Wang F, Wang L, Lv L, Xie Q, et al. Bioinspired protein/peptide loaded 3D printed PLGA scaffold promotes bone regeneration. Front Bioeng Biotechnol. 2022;10:832727. [CrossRef].
98. Choe G, Lee M, Oh S, Seok JM, Kim J, Im S, et al. Three-dimensional bioprinting of mesenchymal stem cells using an osteoinductive bioink containing alginate and BMP-2-loaded PLGA nanoparticles for bone tissue engineering. Biomater Adv. 2022;136:212789. [CrossRef].
99. Johari N, Adabavazeh Z, Baino F. PVA-based bioinks for 3D bioprinting: a comprehensive review of their applications in tissue engineering. Bioprinting. 2025;49:e00419. [CrossRef].
100. Zhang T, Liu H, Nie P, Wang K, Wang X, Liu Y, et al. Enhancement of alginate/gelatin/polyvinyl alcohol hydrogels for multi-crosslinked 3D printed blood vessels. Int J Biol Macromol. 2025;310:142947. [CrossRef].
101. Panieraki A, Mahmoodi N, Anthony C, Dyson RJ, Thomas-Seale LEJ. Exploring the mechanical properties of bioprinted multi-layered polyvinyl alcohol cryogel for vascular applications. J Manuf Mater Process. 2025;9(6):173. [CrossRef].
102. Loukelis K, Kontogianni GI, Vlassopoulos D, Chatzinikolaidou M. Extrusion-based 3D bioprinted gellan gum/poly(vinyl alcohol)/nano-hydroxyapatite composite bioinks promote bone regeneration. Adv Healthc Mater. 2025;14(19):2500365. [CrossRef].
103. Ly M, Spinelli S, Hays S, Zhu D. 3D printing of ceramic biomaterials. Eng Regen. 2022;3(1):41–52. [CrossRef].
104. Khalaf AT, Wei Y, Wan J, Zhu J, Peng Y, Abdul Kadir SY, et al. Bone tissue engineering through 3D bioprinting of bioceramic scaffolds: a review and update. Life. 2022;12(6):903. [CrossRef].
105. Umeyama R, Yamawaki T, Liu D, Kanazawa S, Takato T, Hoshi K, et al. Optimization of culture duration of bone marrow cells before transplantation with a β-tricalcium phosphate/recombinant collagen peptide hybrid scaffold. Regen Ther. 2020;14:284–95. [CrossRef].
106. Awasthi S, Pandey SK, Arunan E, Srivastava C. A review on hydroxyapatite coatings for the biomedical applications: experimental and theoretical perspectives. J Mater Chem B. 2021;9(2):228–49. [CrossRef].
107. Mobaraki M, Ghaffari M, Yazdanpanah A, Luo Y, Mills DK. Bioinks and bioprinting: a focused review. Bioprinting. 2020;18:e00080. [CrossRef].

108. Wenz A, Borchers K, Tovar GEM, Kluger PJ. Bone matrix production in hydroxyapatite-modified hydrogels suitable for bone bioprinting. Biofabrication. 2017;9(4):044103. [CrossRef].
109. Montanari M, Korkeamäki JT, Campodoni E, Mohamed-Ahmed S, Mustafa K, Sandri M, et al. Effects of magnesium-doped hydroxyapatite nanoparticles on bioink formulation for bone tissue engineering. ACS Appl Bio Mater. 2025;8(1):535–47. [CrossRef].
110. Fitzpatrick V, Martín-Moldes Z, Deck A, Torres-Sanchez R, Valat A, Cairns D, et al. Functionalized 3D-printed silk-hydroxyapatite scaffolds for enhanced bone regeneration with innervation and vascularization. Biomaterials. 2021;276:120995. [CrossRef].
111. Xu C, Sun Y, Jansen J, Li M, Wei L, Wu Y, et al. Calcium phosphate ceramics and synergistic bioactive agents for osteogenesis in implant dentistry. Tissue Eng Part C Meth. 2023;29(5):197–215. [CrossRef].
112. Bezerra Melo MC, Spirandeli BR, Barbosa L, Ribeiro dos Santos V, Bastos de Campos TM, Thim GP, et al. Enhanced mechanical strength and bioactivity of 3D-printed β-TCP scaffolds coated with bioactive glasses. J Mech Behav Biomed Mater. 2025;163:106850. [CrossRef].
113. Hesaraki S, Saba G, Shahrezaee M, Nezafati N, Orshesh Z, Roshanfar F, et al. Reinforcing β-tricalcium phosphate scaffolds for potential applications in bone tissue engineering: impact of functionalized multi-walled carbon nanotubes. Sci Rep. 2024;14:19055. [CrossRef].
114. Limlawan P, Insin N, Marger L, Freudenreich M, Durual S, Vacharaksa A. 3D-printed TCP-HA scaffolds delivering microRNA-302a-3p improve bone regeneration in a mouse calvarial model. BDJ Open. 2023;9:50. [CrossRef].
115. El-Rashidy AA, Roether JA, Harhaus L, Kneser U, Boccaccini AR. Regenerating bone with bioactive glass scaffolds: a review of *in vivo* studies in bone defect models. Acta Biomater. 2017;62:1–28. [CrossRef].
116. He L, Yin J, Gao X. Additive manufacturing of bioactive glass and its polymer composites as bone tissue engineering scaffolds: a review. Bioengineering. 2023;10(6):672. [CrossRef].
117. Deliormanlı AM. Novel sol-gel inks for the direct writing of SiO_2-based bioactive glass scaffolds for tissue engineering applications. Silicon. 2025;17(4):775–87. [CrossRef].
118. Hambitzer L, Hornbostel JM, Roolfs L, Prediger R, Kluck S, Zheng K, et al. Bioactive glass microscaffolds fabricated by two-photon lithography. Adv Mater. 2025;37(29):2504475. [CrossRef].
119. Sánchez-Salcedo S, García A, González-Jiménez A, Vallet-Regí M. Antibacterial effect of 3D printed mesoporous bioactive glass scaffolds doped with metallic silver nanoparticles. Acta Biomater. 2023;155:654–66. [CrossRef].
120. Lee SS, Du X, Kim I, Ferguson SJ. Scaffolds for bone-tissue engineering. Matter. 2022;5(9):2722–59. [CrossRef].
121. Ghassemi T, Shahroodi A, Ebrahimzadeh MH, Mousavian A, Movaffagh J, Moradi A. Current concepts in scaffolding for bone tissue engineering. Arch Bone Jt Surg. 2018;6(2):90–9.
122. Ataollahi S. A review on additive manufacturing of lattice structures in tissue engineering. Bioprinting. 2023;35:e00304. [CrossRef].
123. Takizawa T, Nakayama N, Haniu H, Aoki K, Okamoto M, Nomura H, et al. Titanium fiber plates for bone tissue repair. Adv Mater. 2018;30(4):1703608. [CrossRef].
124. Niinomi M, Nakai M, Hieda J. Development of new metallic alloys for biomedical applications. Acta Biomater. 2012;8(11):3888–903. [CrossRef].
125. Geng H, Poologasundarampillai G, Todd N, Devlin-Mullin A, Moore KL, Golrokhi Z, et al. Biotransformation of silver released from nanoparticle coated titanium implants revealed in regenerating bone. ACS Appl Mater Interfaces. 2017;9(25):21169–80. [CrossRef].
126. Shen X, Zhang Y, Ma P, Sutrisno L, Luo Z, Hu Y, et al. Fabrication of magnesium/zinc-metal organic framework on titanium implants to inhibit bacterial infection and promote bone regeneration. Biomaterials. 2019;212:1–16. [CrossRef].
127. Hirota M, Shima T, Sato I, Ozawa T, Iwai T, Ametani A, et al. Development of a biointegrated mandibular reconstruction device consisting of bone compatible titanium fiber mesh scaffold. Biomaterials. 2016;75:223–36. [CrossRef].
128. Kapat K, Srivas PK, Rameshbabu AP, Maity PP, Jana S, Dutta J, et al. Influence of porosity and pore-size distribution in Ti_6Al_4 V foam on physicomechanical properties, osteogenesis, and quantitative validation of bone ingrowth by micro-computed tomography. ACS Appl Mater Interfaces. 2017;9(45):39235–48. [CrossRef].
129. Lin J, Yan A, Huang A, Tang Q, Lu J, Xu H, et al. Nickel–titanium alloy porous scaffolds based on a dominant cellular structure manufactured by laser powder bed fusion have satisfactory osteogenic efficacy. Mater Today Bio. 2024;29:101344. [CrossRef].

130. Jiang H, Cheng P, Li D, Li J, Wang J, Gao Y, et al. Novel standardized massive bone defect model in rats employing an internal eight-hole stainless steel plate for bone tissue engineering. J Tissue Eng Regen Med. 2018;12(4):e2162–71. [CrossRef].
131. Kang HK, Chu TM, Dechow P, Stewart K, Kyung HM, Liu SS. Laser-treated stainless steel mini-screw implants: 3D surface roughness, bone-implant contact, and fracture resistance analysis. Eur J Orthod. 2016;38(2):154–62. [CrossRef].
132. Fan W, Crawford R, Xiao Y. Enhancing *in vivo* vascularized bone formation by cobalt chloride-treated bone marrow stromal cells in a tissue engineered periosteum model. Biomaterials. 2010;31(13):3580–9. [CrossRef].
133. McCarthy EM, Floyd H, Addison O, Zhang ZJ, Oppenheimer PG, Grover LM. Influence of cobalt ions on collagen gel formation and their interaction with osteoblasts. ACS Omega. 2018;3(8):10129–38. [CrossRef].
134. Focaroli S, Teti G, Salvatore V, Orienti I, Falconi M. Calcium/cobalt alginate beads as functional scaffolds for cartilage tissue engineering. Stem Cells Int. 2016;2016:2030478. [CrossRef].
135. Santos de Laia AG, Barrioni BR, Valverde TM, de Goes AM, de Sá MA, de Magalhães Pereira M. Therapeutic cobalt ion incorporated in poly(vinyl alcohol)/bioactive glass scaffolds for tissue engineering. J Mater Sci. 2020;55(20):8710–27. [CrossRef].
136. Islam M, Lantada AD, Mager D, Korvink JG. Carbon-based materials for articular tissue engineering: from innovative scaffolding materials toward engineered living carbon. Adv Healthc Mater. 2022;11:2101834. [CrossRef].
137. Eivazzadeh-Keihan R, Maleki A, de la Guardia M, Bani MS, Chenab KK, Pashazadeh-Panahi P, et al. Carbon based nanomaterials for tissue engineering of bone: building new bone on small black scaffolds: a review. J Adv Res. 2019;18:185–201. [CrossRef].
138. Lopez de Armentia S, del Real JC, Paz E, Dunne N. Advances in biodegradable 3D printed scaffolds with carbon-based nanomaterials for bone regeneration. Materials. 2020;13(22):5083. [CrossRef].
139. Yang W, Li C, Han L. Mechanical properties of polycaprolactone bone scaffolds reinforced with carbon nanotube-modified tricalcium phosphate. Carbon Lett. 2025;35(1):267–76. [CrossRef].
140. Gharivi M, Saraei M, Khachatourian AM, Nemati A, Gholipourmalekabadi M. Fabrication and characterization of functionalized carbon nanotube-reinforced hydroxyapatite/silk fibroin scaffolds for bone tissue engineering applications. Mater Chem Phys. 2025;338:130656. [CrossRef].
141. Zhao Q, Yang D, Chen S, Yang N, Yan T, Lan C, et al. Carbon nanotube bacterial cellulose polycaprolactone scaffolds for bone tissue engineering using top-heating fused deposition three-dimensional printing. Int J Biol Macromol. 2025;318:144588. [CrossRef].
142. Bellet P, Gasparotto M, Pressi S, Fortunato A, Scapin G, Mba M, et al. Graphene-based scaffolds for regenerative medicine. Nanomaterials. 2021;11(2):404. [CrossRef].
143. Meng D, Hou Y, Kurniawan D, Weng RJ, Chiang WH, Wang W. 3D-printed graphene and graphene quantum dot-reinforced polycaprolactone scaffolds for bone-tissue engineering. ACS Appl Nano Mater. 2024;7(1):1245–56. [CrossRef].
144. Diez-Aldama I, Garcia-Villen F, Saenz-del-Burgo L, Scaini D, Pedraz JL. Graphene oxide modified bioink for 3D-bioprinting of vascular graft. ACS Appl Bio Mater. 2025;8(5):3858–72. [CrossRef].
145. Özder MN, Yelkenci A, Kucak M, Altinbay A, Ustündag CB, Ciftci F. Development and characterization of a polycaprolactone/graphene oxide scaffold for *Meniscus* Cartilage regeneration using 3D bioprinting. Pharmaceutics. 2025;17(3):346. [CrossRef].
146. Biegun J. Bio materials for tissue engineering: a comprehensive overview. J Tiss Sci Eng. 2023;14:323.
147. Rasouli R, Sweeney C, Frampton JP. Heterogeneous and composite bioinks for 3D-bioprinting of complex tissue. Biomed Mater Devices. 2025;3(1):108–26. [CrossRef].
148. Cao S, Zhao Y, Hu Y, Zou L, Chen J. New perspectives: *in situ* tissue engineering for bone repair scaffold. Compos Part B Eng. 2020;202:108445. [CrossRef].
149. Motelica L, Oprea O, Ficai D, Ficai A. Introduction to biomaterials and tissue engineering. In: Gunduz O, Egles C, Pérez RA, Ficai D, Ustundag CB, editors. Biomaterials and tissue engineering. Cham, Switzerland: Springer International Publishing; 2023. p. 1–29. [CrossRef].
150. Fontes AB, Marcomini RF. 3D Bioprinting: a review of materials, processes and bioink properties. J Eng Exact Sci. 2020;6(5):617–39. [CrossRef].
151. Bjelić D, Finšgar M. The role of growth factors in bioactive coatings. Pharmaceutics. 2021;13(7):1083. [CrossRef].

152. Nosenko MA, Moysenovich AM, Arkhipova AY, Atretkhany KN, Nedospasov SA, Drutskaya MS, et al. Fibroblasts upregulate expression of adhesion molecules and promote lymphocyte retention in 3D fibroin/gelatin scaffolds. Bioact Mater. 2021;6(10):3449–60. [CrossRef].
153. Nuutila K, Samandari M, Endo Y, Zhang Y, Quint J, Schmidt TA, et al. *In vivo* printing of growth factor-eluting adhesive scaffolds improves wound healing. Bioact Mater. 2022;8:296–308. [CrossRef].
154. Ullah MW, Ul-Islam M, Shehzad A, Manan S, Islam SU, Fatima A, et al. From bioinks to functional tissues and organs: advances, challenges, and the promise of 3D bioprinting. Macro Mater Eng. 2025;310(12):e00251. [CrossRef].
155. Compaired PM, García-Gareta E, Pérez MÁ. An experimental workflow for bioprinting optimization: application to a custom-made biomaterial ink. Int J Bioprinting. 2025:025120094. [CrossRef].
156. Kačarević ŽP, Rider PM, Alkildani S, Retnasingh S, Smeets R, Jung O, et al. An introduction to 3D bioprinting: possibilities, challenges and future aspects. Materials. 2018;11(11):2199. [CrossRef].
157. Zhang J, Wehrle E, Rubert M, Müller R. 3D bioprinting of human tissues: biofabrication, bioinks, and bioreactors. Int J Mol Sci. 2021;22(8):3971. [CrossRef].
158. Gudapati H, Dey M, Ozbolat I. A comprehensive review on droplet-based bioprinting: past, present and future. Biomaterials. 2016;102:20–42. [CrossRef].
159. Xu H, Zhang S, Song K, Yang H, Yin J, Huang Y. Droplet-based 3D bioprinting for drug delivery and screening. Adv Drug Deliv Rev. 2025;217:115486. [CrossRef].
160. Wang Z, Wang L, Li T, Liu S, Guo B, Huang W, et al. 3D bioprinting in cardiac tissue engineering. Theranostics. 2021;11(16):7948–69. [CrossRef].
161. Lee JM, Sing SL, Zhou M, Yeong WY. 3D bioprinting processes: a perspective on classification and terminology. Int J Bioprinting. 2018;4(2):151. [CrossRef].
162. Agarwal T, Fortunato GM, Hann SY, Ayan B, Vajanthri KY, Presutti D, et al. Recent advances in bioprinting technologies for engineering cardiac tissue. Mater Sci Eng C. 2021;124:112057. [CrossRef].
163. Derby B. Bioprinting: inkjet printing proteins and hybrid cell-containing materials and structures. J Mater Chem. 2008;18(47):5717. [CrossRef].
164. Faulkner-Jones A, Greenhough S, A King J, Gardner J, Courtney A, Shu W. Development of a valve-based cell printer for the formation of human embryonic stem cell spheroid aggregates. Biofabrication. 2013;5(1):015013. [CrossRef].
165. Lakkala P, Munnangi SR, Bandari S, Repka M. Additive manufacturing technologies with emphasis on stereolithography 3D printing in pharmaceutical and medical applications: a review. Int J Pharm X. 2023;5:100159. [CrossRef].
166. Zakeri S, Vippola M, Levänen E. A comprehensive review of the photopolymerization of ceramic resins used in stereolithography. Addit Manuf. 2020;35:101177. [CrossRef].
167. Liu J, Miller K, Ma X, Dewan S, Lawrence N, Whang G, et al. Direct 3D bioprinting of cardiac micro-tissues mimicking native myocardium. Biomaterials. 2020;256:120204. [CrossRef].
168. Wu CA, Zhu Y, Woo YJ. Advances in 3D bioprinting: techniques, applications, and future directions for cardiac tissue engineering. Bioengineering. 2023;10(7):842. [CrossRef].
169. Hoffmann A, Leonards H, Tobies N, Pongratz L, Kreuels K, Kreimendahl F, et al. New stereolithographic resin providing functional surfaces for biocompatible three-dimensional printing. J Tissue Eng. 2017;8:2041731417744485. [CrossRef].
170. Li W, Wang M, Ma H, Chapa-Villarreal FA, Lobo AO, Zhang YS. Stereolithography apparatus and digital light processing-based 3D bioprinting for tissue fabrication. iScience. 2023;26(2):106039. [CrossRef].
171. Ning L, Chen X. A brief review of extrusion-based tissue scaffold bio-printing. Biotechnol J. 2017;12(8):1600671. [CrossRef].
172. Ozbolat IT, Hospodiuk M. Current advances and future perspectives in extrusion-based bioprinting. Biomaterials. 2016;76:321–43. [CrossRef].
173. Gillispie G, Prim P, Copus J, Fisher J, Mikos AG, Yoo JJ, et al. Assessment methodologies for extrusion-based bioink printability. Biofabrication. 2020;12(2):022003. [CrossRef].
174. Hölzl K, Lin S, Tytgat L, Van Vlierberghe S, Gu L, Ovsianikov A. Bioink properties before, during and after 3D bioprinting. Biofabrication. 2016;8(3):032002. [CrossRef].

175. Ramesh S, Harrysson OLA, Rao PK, Tamayol A, Cormier DR, Zhang Y, et al. Extrusion bioprinting: recent progress, challenges, and future opportunities. Bioprinting. 2021;21:e00116. [CrossRef].
176. Chang J, Sun X. Laser-induced forward transfer based laser bioprinting in biomedical applications. Front Bioeng Biotechnol. 2023;11:1255782. [CrossRef].
177. Song D, Xu Y, Liu S, Wen L, Wang X. Progress of 3D bioprinting in organ manufacturing. Polymers. 2021;13(18):3178. [CrossRef].
178. Ventura RD. An overview of laser-assisted bioprinting (LAB) in tissue engineering applications. Med Lasers. 2021;10(2):95–118. [CrossRef].
179. Dou C, Perez V, Qu J, Tsin A, Xu B, Li J. A state-of-the-art review of laser-assisted bioprinting and its future research trends. ChemBioEng Rev. 2021;8(5):517–34. [CrossRef].
180. Bishop ES, Mostafa S, Pakvasa M, Luu HH, Lee MJ, Wolf JM, et al. 3-D bioprinting technologies in tissue engineering and regenerative medicine: current and future trends. Genes Dis. 2017;4(4):185–95. [CrossRef].
181. Guillotin B, Ali M, Ducom A, Catros S, Keriquel V, Souquet A, et al. Laser-assisted bioprinting for tissue engineering. In: Forgacs G, Sun W, editors. Biofabrication. Boston, MA, USA: William Andrew Publishing; 2013. p. 95–118. [CrossRef].
182. Elango J, Lijnev A, Zamora-Ledezma C, Alexis F, Wu W, Marín JMG, et al. The relationship of rheological properties and the performance of silk fibroin hydrogels in tissue engineering application. Process Biochem. 2023;125:198–211. [CrossRef].
183. Cowie JMG, Arrighi V. Rheology and mechanical properties in polymers: chemistry and physics of modern materials. Boca Raton, FL, USA: CRC Press; 2007. [CrossRef].
184. De Smedt S, Attaianese B, Cardinaels R. Direct ink writing of particle-based multiphase materials: from rheology to functionality. Curr Opin Colloid Interface Sci. 2025;75:101889. [CrossRef].
185. Schwab A, Levato R, D'Este M, Piluso S, Eglin D, Malda J. Printability and shape fidelity of bioinks in 3D bioprinting. Chem Rev. 2020;120(19):11028–55. [CrossRef].
186. Chen DTN, Wen Q, Janmey PA, Crocker JC, Yodh AG. Rheology of soft materials. Annu Rev Condens Matter Phys. 2010;1:301–22. [CrossRef].
187. Ji S, Guvendiren M. Recent advances in bioink design for 3D bioprinting of tissues and organs. Front Bioeng Biotechnol. 2017;5:23. [CrossRef].
188. Elango J, Zamora-Ledezma C. Rheological, structural, and biological trade-offs in bioink design for 3D bioprinting. Gels. 2025;11(8):659. [CrossRef].
189. Kitana W, Levario-Diaz V, Cavalcanti-Adam EA, Ionov L. Biofabrication of composite bioink-nanofiber constructs: effect of rheological properties of bioinks on 3D (bio)printing and cells interaction with aligned touch spun nanofibers. Adv Healthc Mater. 2024;13(6):2303343. [CrossRef].
190. Bercea M. Rheology as a tool for fine-tuning the properties of printable bioinspired gels. Molecules. 2023;28(6):2766. [CrossRef].
191. Tan B, Gan S, Wang X, Liu W, Li X. Applications of 3D bioprinting in tissue engineering: advantages, deficiencies, improvements, and future perspectives. J Mater Chem B. 2021;9(27):5385–413. [CrossRef].
192. Yi HG, Kim H, Kwon J, Choi YJ, Jang J, Cho DW. Application of 3D bioprinting in the prevention and the therapy for human diseases. Sig Transduct Target Ther. 2021;6:177. [CrossRef].
193. Zhou X, Zhu W, Nowicki M, Miao S, Cui H, Holmes B, et al. 3D bioprinting a cell-laden bone matrix for breast cancer metastasis study. ACS Appl Mater Interfaces. 2016;8(44):30017–26. [CrossRef].
194. Zhu W, Holmes B, Glazer RI, Zhang LG. 3D printed nanocomposite matrix for the study of breast cancer bone metastasis. Nanomed Nanotechnol Biol Med. 2016;12(1):69–79. [CrossRef].
195. Dixon DT, Landree EN, Gomillion CT. 3D-printed demineralized bone matrix-based conductive scaffolds combined with electrical stimulation for bone tissue engineering applications. ACS Appl Bio Mater. 2024;7(7):4366–78. [CrossRef].
196. Rindone AN, Nyberg E, Grayson WL. 3D-printing composite polycaprolactone-decellularized bone matrix scaffolds for bone tissue engineering applications. Methods Mol Biol. 2018;1577:209–26. [CrossRef].
197. Seo Lee J, Nah H, Lee D, An SH, Ko WK, Lee S, et al. Immediately implantable extracellular matrix-enriched osteoinductive hydrogel-laden 3D-printed scaffold for promoting vascularized bone regeneration *in vivo*. Mater Des. 2022;219:110801. [CrossRef].

198. Vázquez-Aristizabal P, Henriksen-Lacey M, García-Astrain C, Jimenez de Aberasturi D, Langer J, Epelde C, et al. Biofabrication and monitoring of a 3D printed skin model for melanoma. Adv Healthc Mater. 2024;13(27):2401136. [CrossRef].
199. Wang Y, Gao C, Cheng S, Li Y, Huang Y, Cao X, et al. 3D bioprinting of double-layer conductive skin for wound healing. Adv Healthc Mater. 2025;14(9):2404388. [CrossRef].
200. Liu P, Shen H, Zhi Y, Si J, Shi J, Guo L, et al. 3D bioprinting and *in vitro* study of bilayered membranous construct with human cells-laden alginate/gelatin composite hydrogels. Colloids Surf B Biointerfaces. 2019;181:1026–34. [CrossRef].
201. Hafezi F, Shorter S, Tabriz AG, Hurt A, Elmes V, Boateng J, et al. Bioprinting and preliminary testing of highly reproducible novel bioink for potential skin regeneration. Pharmaceutics. 2020;12(6):550. [CrossRef].
202. Zou Q, Tian X, Luo S, Yuan D, Xu S, Yang L, et al. Agarose composite hydrogel and PVA sacrificial materials for bioprinting large-scale, personalized face-like with nutrient networks. Carbohydr Polym. 2021;269:118222. [CrossRef].
203. Miguel SP, Cabral CSD, Moreira AF, Correia IJ. Production and characterization of a novel asymmetric 3D printed construct aimed for skin tissue regeneration. Colloids Surf B Biointerfaces. 2019;181:994–1003. [CrossRef].
204. Lee A, Hudson AR, Shiwarski DJ, Tashman JW, Hinton TJ, Yerneni S, et al. 3D bioprinting of collagen to rebuild components of the human heart. Science. 2019;365(6452):482–7. [CrossRef].
205. Esser TU, Anspach A, Muenzebrock KA, Kah D, Schrüfer S, Schenk J, et al. Direct 3D-bioprinting of hiPSC-derived cardiomyocytes to generate functional cardiac tissues. Adv Mater. 2023;35(52):2305911. [CrossRef].
206. Hwang DG, Choi H, Yong U, Kim D, Kang W, Park SM, et al. Bioprinting-assisted tissue assembly for structural and functional modulation of engineered heart tissue mimicking left ventricular myocardial fiber orientation. Adv Mater. 2024;36(34):2400364. [CrossRef].
207. Ma X, Dewan S, Liu J, Tang M, Miller KL, Yu C, et al. 3D printed micro-scale force gauge arrays to improve human cardiac tissue maturation and enable high throughput drug testing. Acta Biomater. 2019;95:319–27. [CrossRef].
208. Izadifar M, Chapman D, Babyn P, Chen X, Kelly ME. UV-assisted 3D bioprinting of nanoreinforced hybrid cardiac patch for myocardial tissue engineering. Tissue Eng Part C Meth. 2018;24(2):74–88. [CrossRef].
209. Khati V, Ramachandraiah H, Pati F, Svahn HA, Gaudenzi G, Russom A. 3D bioprinting of multi-material decellularized liver matrix hydrogel at physiological temperatures. Biosensors. 2022;12(7):521. [CrossRef].
210. He J, Wang J, Pang Y, Yu H, Qin X, Su K, et al. Bioprinting of a hepatic tissue model using HumanInduced pluripotent stem cell-derived hepatocytes for drug-induced hepatotoxicity evaluation. Int J Bioprinting. 2022;8(3):581. [CrossRef].
211. Cuvellier M, Ezan F, Oliveira H, Rose S, Fricain JC, Langouët S, et al. 3D culture of HepaRG cells in GelMa and its application to bioprinting of a multicellular hepatic model. Biomaterials. 2021;269:120611. [CrossRef].
212. Janani G, Priya S, Dey S, Mandal BB. Mimicking native liver lobule microarchitecture *in vitro* with parenchymal and non-parenchymal cells using 3D bioprinting for drug toxicity and drug screening applications. ACS Appl Mater Interfaces. 2022;14(8):10167–86. [CrossRef].
213. Hong G, Kim J, Oh H, Yun S, Kim CM, Jeong YM, et al. Production of multiple cell-laden microtissue spheroids with a biomimetic hepatic-lobule-like structure. Adv Mater. 2021;33(36):2102624. [CrossRef].
214. Phogat S, Guo TJF, Thiam F, Osei ET. Establishing a 3D vascularized tri-culture model of the human airways via a digital light processing bioprinter. Biotech Bioeng. 2025;122(8):2273–80. [CrossRef].
215. Wan W, Wang X, Zhang R, Li Y, Wu H, Liu Y, et al. Construction of artificial lung tissue structure with 3D-inkjet bioprinting core for pulmonary disease evaluation. J Tissue Eng. 2025;16:20417314251328128. [CrossRef].
216. Kang D, Park JA, Kim W, Kim S, Lee HR, Kim WJ, et al. All-inkjet-printed 3D alveolar barrier model with physiologically relevant microarchitecture. Adv Sci. 2021;8(10):2004990. [CrossRef].
217. Yeh YC, Chen PY, Chen KT, Lee IC. Innovative MXene/SilMA-based conductive bioink for three dimensional bioprinting of neural stem cell spheroids in neural tissue engineering. ACS Appl Mater Interfaces. 2025;17(7):10402–16. [CrossRef].
218. Ma H, de Oliveira Ferreira R, de Oliveira D, Endo A, Okamoto OK, Zatz M. Enhanced integration of *ex vivo* lesioned brain via 3D bioprinted neural progenitor cell constructs promote neuronal differentiation. Cytotherapy. 2025;27(5):S107. [CrossRef].
219. Liu X, Hao M, Chen Z, Zhang T, Huang J, Dai J, et al. 3D bioprinted neural tissue constructs for spinal cord injury repair. Biomaterials. 2021;272:120771. [CrossRef].

220. Dell AC, Maresca J, Davis BA, Isaji T, Dardik A, Geibel JP. Development and deployment of a functional 3D-bioprinted blood vessel. Sci Rep. 2025;15:11668. [CrossRef].
221. Ajji Z, Jafari A, Mousavi A, Ajji A, Heuzey MC, Savoji H. 3D bioprinting of thick core–shell vascularized scaffolds for potential tissue engineering applications. Eur Polym J. 2025;222:113564. [CrossRef].
222. Zhu J, Ma H, Du J, Fang H, Cheng YY, Xu J, et al. A coaxial 3D bioprinted hybrid vascular scaffold based on decellularized extracellular matrix/nano clay/sodium alginate bioink. Int J Biol Macromol. 2025;290:139056. [CrossRef].
223. Nonaka T, Murata D, Yoshizato H, Kashimoto S, Nakamura A, Morimoto T, et al. Bio-3D printing of scaffold-free ADSC-derived cartilage constructs comparable to natural cartilage *in vitro*. J Orthop Surg Res. 2025;20(1):182. [CrossRef].
224. Di Gesù R, Palumbo Piccionello A, Vitale G, Buscemi S, Panzavolta S, Di Filippo MF, et al. Biofabrication of an *in situ* hypoxia-delivery scaffold for cartilage regeneration. Biofabrication. 2025;17(2):025025. [CrossRef].
225. Ci Z, Huo Y, Tang B, Li G, Jia Z, Zhang P, et al. Micro-structure modified decalcified bone matrix scaffolds and bone marrow stem cell–chondrocyte co-cultures promote stable cartilage regeneration. Compos Part B Eng. 2025;291:111976. [CrossRef].
226. McMillan A, Hoffman MR, Xu Y, Wu Z, Thayer E, Peel A, et al. 3D bioprinted ferret mesenchymal stem cell-laden cartilage grafts for laryngotracheal reconstruction in a ferret surgical model. Biomater Sci. 2025;13(5):1304–22. [CrossRef].
227. Nguyen LH, Kudva AK, Saxena NS, Roy K. Engineering articular cartilage with spatially-varying matrix composition and mechanical properties from a single stem cell population using a multi-layered hydrogel. Biomaterials. 2011;32(29):6946–52. [CrossRef].
228. Shim JH, Kim JY, Park M, Park J, Cho DW. Development of a hybrid scaffold with synthetic biomaterials and hydrogel using solid freeform fabrication technology. Biofabrication. 2011;3(3):034102. [CrossRef].
229. Ahn G, Min KH, Kim C, Lee JS, Kang D, Won JY, et al. Precise stacking of decellularized extracellular matrix based 3D cell-laden constructs by a 3D cell printing system equipped with heating modules. Sci Rep. 2017;7:8624. [CrossRef].
230. Shin J, Tabatabaei Rezaei N, Choi S, Li Z, Kim DH, Kim K. Photocrosslinkable kidney decellularized extracellular matrix-based bioink for 3D bioprinting. Adv Healthc Mater. 2025;14(24):2501616. [CrossRef].
231. Dahlan NA, Chiok KLR, Tabil XL, Duan X, Banerjee A, Dhar N, et al. Development and characterization of a decellularized lung ECM-based bioink for bioprinting and fabricating a lung model. Biomater Adv. 2025;177:214428. [CrossRef].
232. Yeleswarapu S, Dash A, Chameettachal S, Pati F. 3D bioprinting of tissue constructs employing dual crosslinking of decellularized extracellular matrix hydrogel. Biomater Adv. 2023;152:213494. [CrossRef].
233. Zhang H, Wang Y, Zheng Z, Wei X, Chen L, Wu Y, et al. Strategies for improving the 3D printability of decellularized extracellular matrix bioink. Theranostics. 2023;13(8):2562–87. [CrossRef].
234. Cohen R, Baruch ES, Cabilly I, Shapira A, Dvir T. Modified ECM-based bioink for 3D printing of multi-scale vascular networks. Gels. 2023;9(10):792. [CrossRef].
235. Behan K, Dufour A, Garcia O, Kelly D. Methacrylated cartilage ECM-based hydrogels as injectables and bioinks for cartilage tissue engineering. Biomolecules. 2022;12(2):216. [CrossRef].
236. Mohanty S, Roy S. Bioactive hydrogels inspired by laminin: an emerging biomaterial for tissue engineering applications. Macromol Biosci. 2024;24(11):2400207. [CrossRef].
237. Ribezzi D, Català P, Pignatelli C, Citro A, Levato R. Bioprinting and synthetic biology approaches to engineer functional endocrine pancreatic constructs. Trends Biotechnol. 2025;43(9):2133–49. [CrossRef].
238. Aizarna-Lopetegui U, Herrero-Ruiz A, Decarli MC, Urigoitia-Asua A, Chavarri-Urraca K, Moroni L, et al. The route to artery mimetics: hybrid bioinks for embedded bioprinting of multimaterial cylindrical models. Adv Funct Materials. 2025;35(49):e19072. [CrossRef].
239. Montero FE, Rezende RA, da Silva JVL, Sabino MA. Development of a smart bioink for bioprinting applications. Front Mech Eng. 2019;5:56. [CrossRef].
240. Castro NJ, Meinert C, Levett P, Hutmacher DW. Current developments in multifunctional smart materials for 3D/4D bioprinting. Curr Opin Biomed Eng. 2017;2:67–75. [CrossRef].
241. de León EH, Valle-Pérez AU, Khan ZN, Hauser CAE. Intelligent and smart biomaterials for sustainable 3D printing applications. Curr Opin Biomed Eng. 2023;26:100450. [CrossRef].

242. Salama AH. Recent advances in 3D and 4D printing in pharmaceutical technology: applications, challenges, and future perspectives. Future J Pharm Sci. 2025;11(1):107. [CrossRef].
243. Zeng J, Li Y, Ma Z, Hu M. Advances in small molecules in cellular reprogramming: effects, structures, and mechanisms. Curr Stem Cell Res Ther. 2021;16(2):115–32. [CrossRef].
244. He X, Liang J, Paul C, Huang W, Dutta S, Wang Y. Advances in cellular reprogramming-based approaches for heart regenerative repair. Cells. 2022;11(23):3914. [CrossRef].
245. Ding S. Therapeutic reprogramming toward regenerative medicine. Chem Rev. 2025;125(4):1805–22. [CrossRef].
246. Heo JH, Kim MK, Lee SJ, Kang HW. Enhanced exosome production in mesenchymal stem cells via extracellular matrix-incorporated 3D spheroid printing. Adv NanoBiomed Res. 2025;5(10):2500007. [CrossRef].
247. Galocha-León C, Antich C, Voltes-Martínez A, Marchal JA, Mallandrich M, Halbaut L, et al. Human mesenchymal stromal cells-laden crosslinked hyaluronic acid-alginate bioink for 3D bioprinting applications in tissue engineering. Drug Deliv Transl Res. 2025;15(1):291–311. [CrossRef].
248. Li G, He J, Shi J, Li X, Liu L, Ge X, et al. Bioprinting functional hepatocyte organoids derived from human chemically induced pluripotent stem cells to treat liver failure. Gut. 2025;74(7):1150–64. [CrossRef].
249. Robinson MA, Kung SH, Youssef KY, Scheck KM, Bell RH, Sar F, et al. 3D bioprinted coaxial testis model using human induced pluripotent stem cells: a step toward bicompartmental cytoarchitecture and functionalization. Adv Healthc Mater. 2025;14(10):2402606. [CrossRef].
250. Du B, Dai Z, Wang H, Ren Z, Li D. Advances and prospects in using induced pluripotent stem cells for 3D bioprinting in cardiac tissue engineering. Rev Cardiovasc Med. 2025;26(3):26697. [CrossRef].
251. Hashimoto S, Taniguchi D, Doi R, Obata T, Shiraishi T, Matsumoto T, et al. Bio-3D printing with smooth muscle cells derived from human iPSCs via neural crest and its application for the tracheal regeneration. Biofabrication. 2026;18(1):015003. [CrossRef].
252. Richards C, Chen H, O'Rourke M, Bannister A, Owen G, Volkerling A, et al. Matrix directs trophoblast differentiation in a bioprinted organoid model of early placental development. Nat Commun. 2025;16:8267. [CrossRef].
253. Paduszyński P, Włodarczyk J, Rok J, Pastusiak M, Rzepka Z, Ochab A, et al. Evaluation of different geometry poly(L-lactide-co-glycolide-co-trimethylene carbonate oligomer) scaffolds fabricated by material extrusion 3D printing for adipose derived stem cells culture. J Biomed Mater Res B Appl Biomater. 2025;113(5):e35580. [CrossRef].
254. Kim W, Hwangbo H, Heo G, Ryu D, Kim G. Enhanced myogenic differentiation of human adipose-derived stem cells via integration of 3D bioprinting and *in situ* shear-based blade coating. Adv Funct Materials. 2025;35:2406591. [CrossRef].
255. Bertassoni LE, Cecconi M, Manoharan V, Nikkhah M, Hjortnaes J, Cristino AL, et al. Hydrogel bioprinted microchannel networks for vascularization of tissue engineering constructs. Lab Chip. 2014;14(13):2202–11. [CrossRef].
256. Miao X, Chen T, Lang Z, Wu Y, Wu X, Zhu Z, et al. Design, fabrication, and application of bioengineering vascular networks based on microfluidic strategies. J Mater Chem B. 2025;13(4):1252–69. [CrossRef].
257. Barua R, Datta S, Das D, Sarkar S, Biswas N. Recent advances in the fabrication of vascularized tissues and blood vessels: a state-of-the-art review. Phys Fluids. 2025;37(10):101301. [CrossRef].
258. Poldervaart MT, Gremmels H, van Deventer K, Fledderus JO, Öner FC, Verhaar MC, et al. Prolonged presence of VEGF promotes vascularization in 3D bioprinted scaffolds with defined architecture. J Control Release. 2014;184:58–66. [CrossRef].
259. Kawai T. Preclinical evaluation and advancements in vascularized bone tissue engineering. Biomimetics. 2025;10(7):412. [CrossRef].
260. Buckley C, Ibrahim R, Giordano F, Xu N, Sems B, Wang H. Sacrificial strategy towards the formation of vascular-like networks in volumetric tissue constructs. BMEMat. 2025;3(2):e12118. [CrossRef].
261. Liu S, Feng K, Teng Z, Zhao R, Kang X, Chen Q, et al. Perfusable and toughening cardiac patch with hierarchically branched microchannels for myocardial infarction revascularization. Mater Horiz. 2025;12(17):6831–41. [CrossRef].
262. Revokatova D, Bikmulina P, Heydari Z, Solovieva A, Vosough M, Shpichka A, et al. Getting blood out of a stone: vascularization via spheroids and organoids in 3D bioprinting. Cells. 2025;14(9):665. [CrossRef].

263. Cai B, Kilian D, Ghorbani S, Roth JG, Seymour AJ, Brunel LG, et al. One-step bioprinting of endothelialized, self-supporting arterial and venous networks. Biofabrication. 2025;17(2):025012. [CrossRef].
264. Gungor-Ozkerim PS, Inci I, Zhang YS, Khademhosseini A, Dokmeci MR. Bioinks for 3D bioprinting: an overview. Biomater Sci. 2018;6(5):915–46. [CrossRef].
265. Wei Q, An Y, Li M, Zhao X. Research on the flow behavior of bio-ink inside the extrusion nozzle during printing. J Appl Phys. 2024;136(17):174701. [CrossRef].
266. Chen XB, Fazel Anvari-Yazdi A, Duan X, Zimmerling A, Gharraei R, Sharma NK, et al. Biomaterials/bioinks and extrusion bioprinting. Bioact Mater. 2023;28:511–36. [CrossRef].
267. Pawar A, Chaudhari A, Immonen E. Analysis of flow behavior of bioinks outside the 3D-printing nozzles. RakMek. 2025;58(4):186–96. [CrossRef].
268. Wei P, Cipriani C, Hsieh CM, Kamani K, Rogers S, Pentzer E. Go with the flow: rheological requirements for direct ink write printability. J Appl Phys. 2023;134(10):100701. [CrossRef].
269. Habib MA, Khoda B. Rheological analysis of bio-ink for 3D bio-printing processes. J Manuf Process. 2022;76:708–18. [CrossRef].
270. Calafel MI, Criado-Gonzalez M, Aguirresarobe R, Fernández M, Mijangos C. From rheological concepts to additive manufacturing assessment of hydrogel-based materials for advanced bioprinting applications. Mater Adv. 2025;6(14):4566–97. [CrossRef].
271. Chand R, Kamei KI, Vijayavenkataraman S. Advances in microfluidic bioprinting for multi-material multi-cellular tissue constructs. CTE Connect. 2025;1(1):1–10. [CrossRef].